Presentation to the NESC Sensors & Instrumentation Discipline
February 20, 2024. Pasadena, California

How Type-II Superlattice (T2SL) Focal Planes have Changed the Infrared Landscape

Sarath Gunapala, David Ting, Sir Rafol, Alexander Soibel, Arezou Khoshakhlagh, Sam Keo, Brian Pepper, Anita Fisher, Cory Hill, William Johnson, Simon Hook, Olga Kalashnikova, Michael Garay, Ashley Davies, Yuki Maruyama, Mehmet Ogut, John Liu, Linda Hoeglund, Frank Greer, Jean Nguyen, Jason Mumolo, and Layton Baker
Jet Propulsion Laboratory, California Institute of Technology

Ashok Sood and John Zeller
Magnolia Optical Technologies, Inc.

Paul Lucey, Robert Wright, Miguel Nunes, and Luke Flynn
Hawai'i Institute of Geophysics and Planetology, University of Hawai'i at Manoa

Sachidananda Babu and Parminder Ghuman
NASA Earth Science Technology Office

Sponsors: NASA, MDA, VISTA, NASA ESTO’s ACT, SLI-T, InVEST, and IIP programs

Outline

- Science rational for infrared R&D

- What led to the sustainable T2SL infrared focal plane array business

Science Rationale

Jet Propulsion Laboratory
California Institute of Technology

Science Rationale

- Land surface temperature (vegetation, soil, snow), at agricultural or topographic scales - thermal infrared, in 4 μm and 11 μm spectral regions, multiple platforms

- Vapor pressure deficit in boundary layer - microwave & IR sounders

- Radiative flux, albedo of snow separately from vegetation and soil, and surface temperature of the snow, at topographic scale - imaging spectrometer thermal infrared, in 4 μm and 11 μm spectral regions

- Wildland fire detection, Quantify the flow of carbon in terrestrial ecosystems, Discover cascading perturbations in ecosystems related to carbon storage, Understand ecosystem response to fire events, Understand how the threat of wildfires is changing with time and how exposure to emissions from wildfires can affect human health – unsaturable (very high dynamic range) 1-5 μm and 8-11μm multiband infrared imagers

- Monitor Global Hydrological Cycles and Water Resources, Provide information for detailed understanding of the movement, distribution & availability of water, and distribution of land surface temperature (LST), Investigate the following global food and water security issues: Mapping both irrigated and rainfed cropland areas; Determining crop water use (actual evapotranspiration (ET)) of major world crops, Establishing crop water productivity ("crop per drop") of major world crops – 8-12 μm hyperspectral imagers

- Sustainable land imaging (Landsat) - 8-12.5 μm broadband focal plane arrays

- Understand eruption mechanisms of Io's volcanoes, Determine the lava eruption temperature and lava composition remotely during Io flybys, Infer Io's interior structure and test internal heating models – 1-10 μm multiband unsaturable imagers

Introduction

Discovery of Infrared

http://coolcosmos.ipac.caltech.edu/cosmic_classroom/ir_tutorial/discovery.html

http://en.wikipedia.org/wiki/William_Herschel

- Sir Frederick William Herschel
  - Musician and composer
  - Built and sold large telescopes
  - Discovered Uranus and 2 of its moons; 2 Saturn moons; double stars
  - Surveyed and catalogued deep sky objects – nebulae, clusters
- Discovered infrared on Feb. 11, 1800
  - Testing filters for sunspot observations
    - Red filter retained more heat
  - Passed sunlight through prism
  - Measured temperatures for color spectrum
    - Increasing from violet to red
  - Placed thermometer just beyond red; showed higher temperature than visible!
  - Invisible form of light – "calorific rays"
    - Reflected, refracted, absorbed, transmitted
  - Postscript: Led to discovery of ultra-violet light by Johann Ritter in 1801
    - "Chemical rays" (reaction in silver chloride)

Atmospheric Transmittance and Infrared Bands

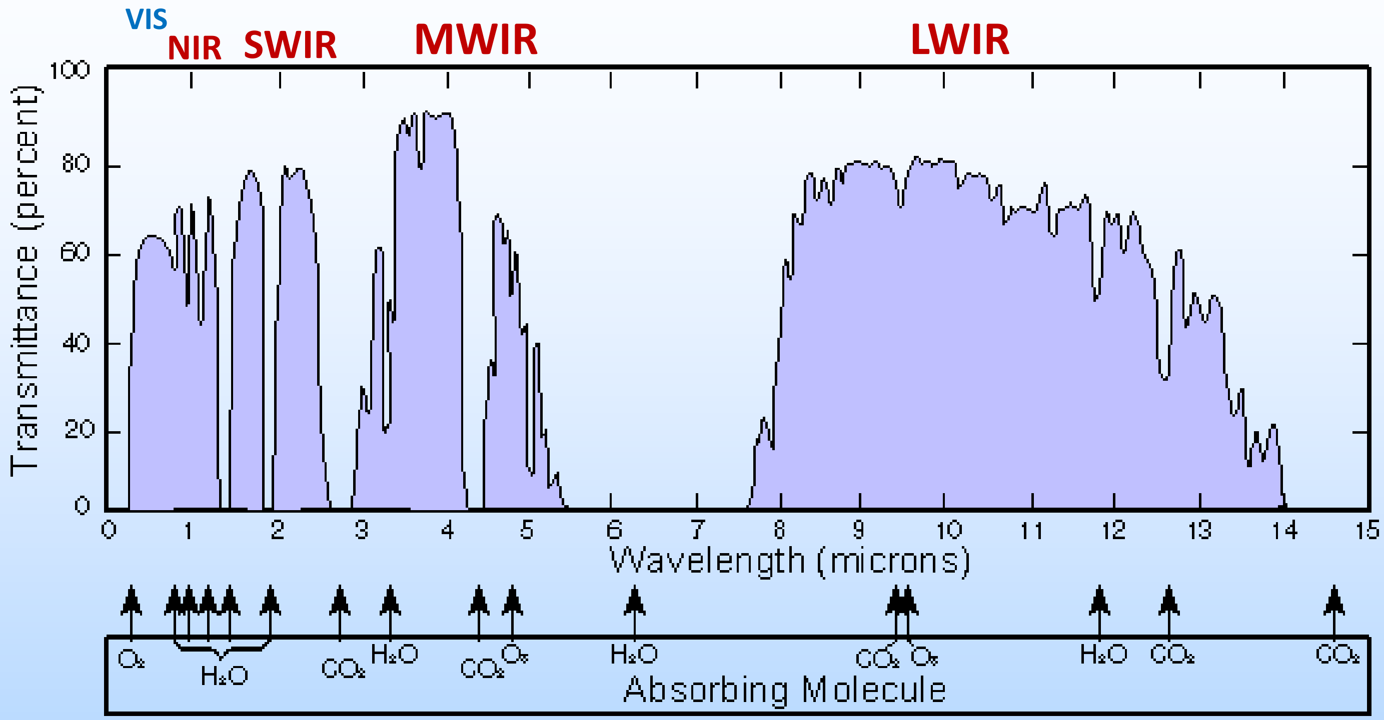

http://en.wikipedia.org/wiki/Infrared

- Near-infrared (NIR): 0.75 – 1.7 µm
- Short-wavelength infrared (SWIR): 1.7 - 3 µm
- Mid-wavelength infrared (MWIR): 3 – 5.5 µm
- Long-wavelength infrared (LWIR): 8 - 12 µm
- Beyond: Very Long-wavelength infrared (VLWIR), Far IR (FIR)
- Different convention for Astronomy: Near-IR, Mid-IR, Far-IR

Common Sources of Infrared Light

- Reflected infrared
  - Like reflected visible light
  - Sunlight (NIR, SWIR)
    - Solar spectrum at sea level: 4% UV, 44% Visible, 52% IR
  - Airglow/Atmospheric Nightglow (SWIR)
    - Night time emission from the Earth's upper atmosphere
    - Mostly in SWIR
- Emitted infrared
  - Blackbody radiation (MWIR, LWIR)
    - 300K BB spectral peak ~9.7 μm

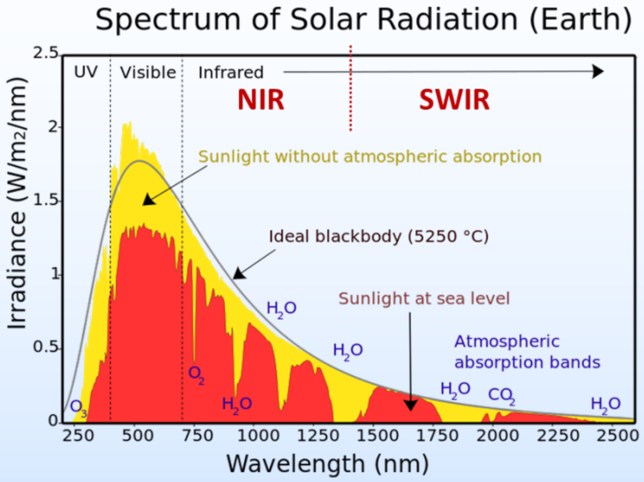

http://commons.wikimedia.org/wiki/File:Solar_spectrum_ita.svg; By Nick84 [CC BY-SA 3.0 (http://creativecommons.org/licenses/by-sa/3.0)], via Wikimedia Commons

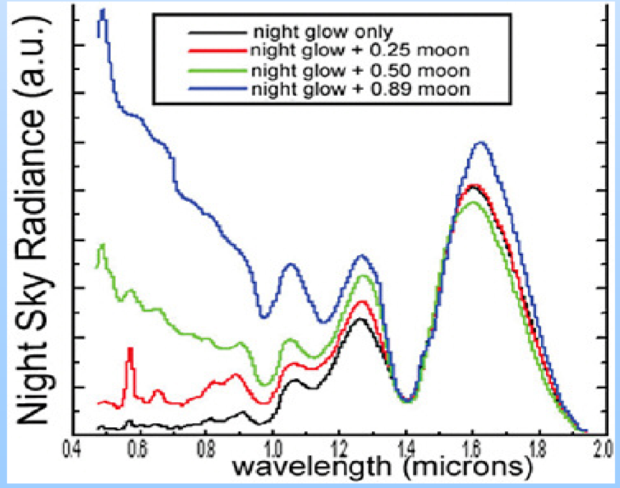

SOURCE: Vatsia, L.M. 1972. Atmospheric optical environment. Research and Development Technical Report ECOM-7023. Prepared for the Army Night Vision Lab, Fort Belvoir, Va.

A Variety of Infrared Detector

This presentation

Past JPL work

Norton's Law:

"All physical phenomena in the range of 0.1-1 eV will be proposed as an infrared detector"

- Thermocouples
- Golay cells - past
- Photon drag effect
- Quantum wells – past (SRTV-1D, Landsat 8, 9, HyTES)
- Superlattices – this presentation
- Josephson junctions
- SQUIDs
- Ballistic electron transistors
- Quantum dots
- Protein microbolometers
- Giant magnetoresistance
- Quantum entanglement
- Polyvinylidene fluoride
- Ferro- and pyro-electrics
- Antenna-coupled Shottky diodes
- Metal-semiconductor-metal junctions
- Resonant tunneling diodes
- Thallium-indium-phosphide/arsenide
- Bimaterial cantilevers
- Nanowires
- Organic semiconductors
- Nanotubes/ Graphene
- Bose-Einstein condensates

Paul Norton Seminar, "Infrared Detectors", Rochester Institute of Technology, April 22, 2010

Commercially Available Infrared Detectors

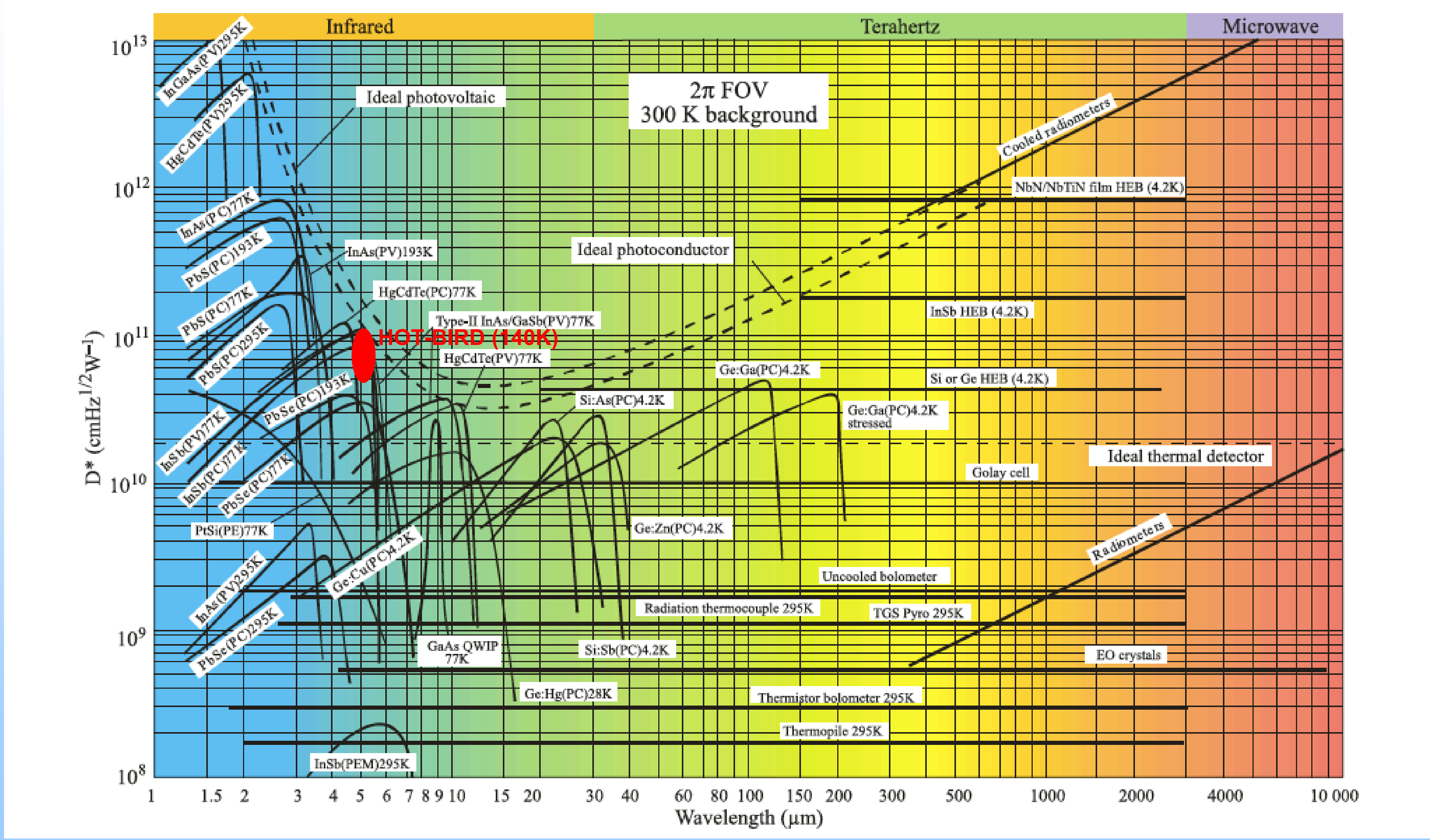

Chopping frequency is 1000 Hz for all detectors except for thermal detectors (i.e., bolometer, thermopile, etc.)

Reference: Infrared Detectors, Antoni Rogalski, CRC Press, Taylor and Francis Group, ISBN 978-1-4200-7671-4

T2SLS Detector Technology

In the Beginning …

- Proposal of superlattices and quantum wells in 1977
  - D. L. Smith and C. Mailhiot, Appl. Phys. Lett. 34(10), 663–665, 1987.

- First demonstration of infrared detection using superlattices in 1990
  - R. H. Miles *et al.*, Appl. Phys. Lett. 57(8), 801–803, 1990.
  - F. Fuchs *et al.*, Appl. Phys. Letts. 73(25), 3760–3762, 1998.
  - Mohseni, H., Michel, E., Razeghi, 30-37, SPIE 3287, 1998.
  - D. Z.-Y. Ting, et al., Appl. Phys. Lett. 95, 023508, 2009.
  - David Z. Ting, et al., US Patent No. US 8,217,480 B2, 2012.

Antimonides Material System for Type-II Superlattices

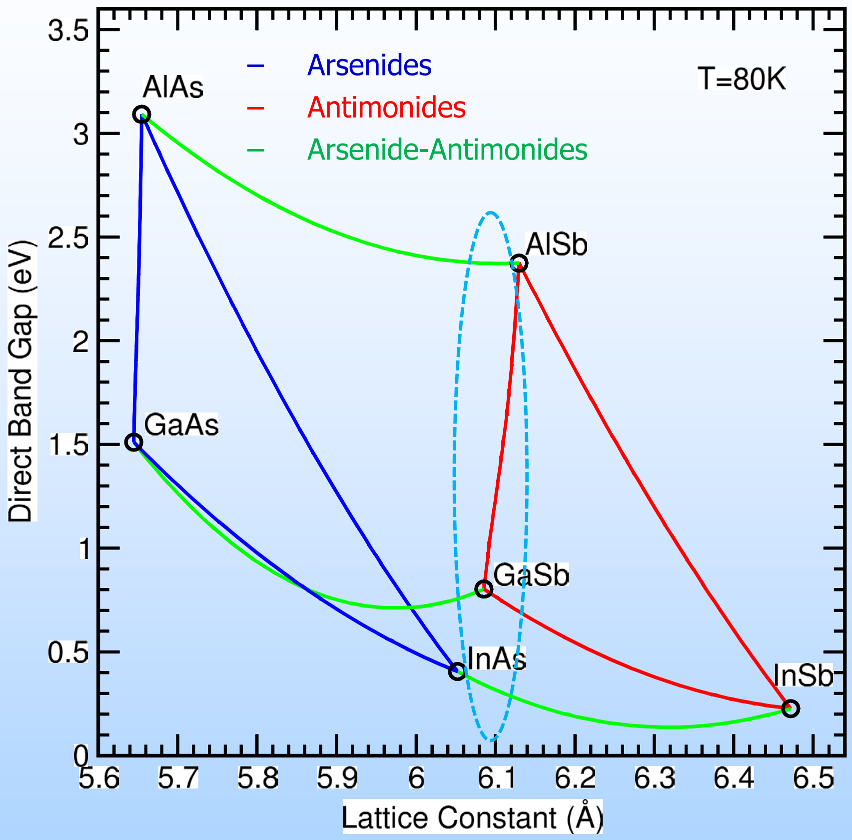

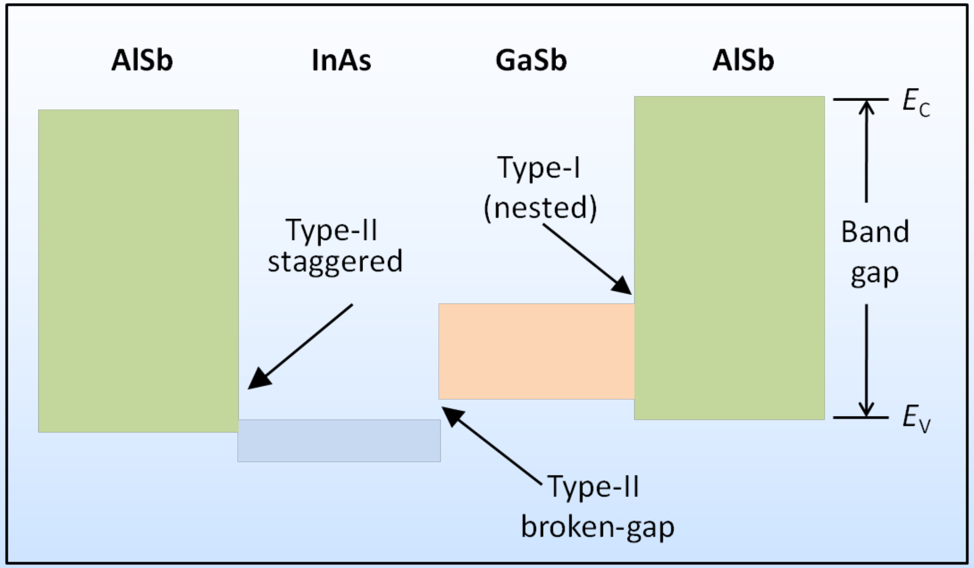

- Material system includes InAs, GaSb, AlSb and their alloys
  - Nearly lattice matched (~6.1 Å)
- Alloys with GaAs, AlAs, and InSb adds even more flexibility

- Three types of band alignments
  - Type-I (nested, straddling)
  - Type-II staggered
  - Type-II broken gap (misaligned, Type-III)
    - Unique among common semiconductor families
    - Overlap between InAs CB and GaSb VB enables interband devices
- Tremendous flexibility in artificially designed materials / device structures

Basic Properties of InAs/Ga(In)Sb Type-II Superlattice

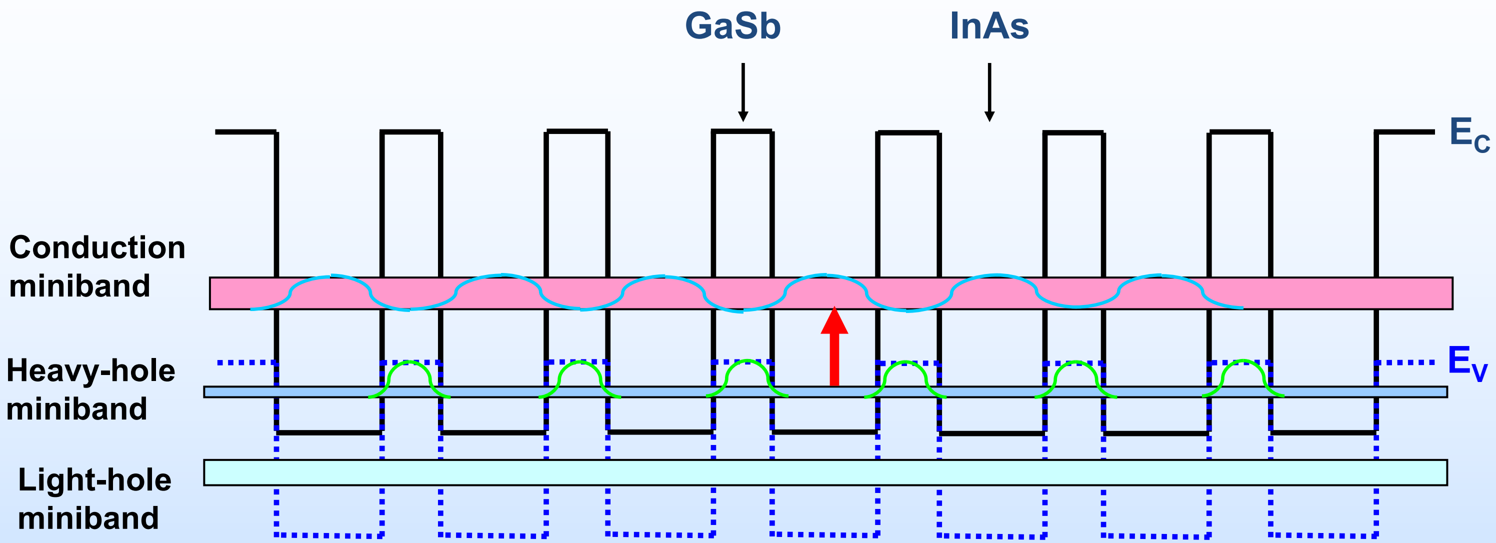

- Type-II broken-gap superlattice (A superlattice is a periodic structure of layers of two (or more) materials. Typically, the thickness of one layer is several nanometers. It can also refer to a lower-dimensional structure such as an array of quantum dots or quantum wells)
  - Spatially separated CB and VB wave functions
    - Reduced oscillator strength (compensated by larger VB edge density of states)
  - Type-II SL band gap is smaller than band gap of either bulk semiconductors
    - Type-I SL band gap always larger than the smaller bulk band gap
  - Nearly independent control of conduction and valence sub-band edges
    - Important for manipulating band alignments

Dark Current Mechanisms in a Homojunction Diode

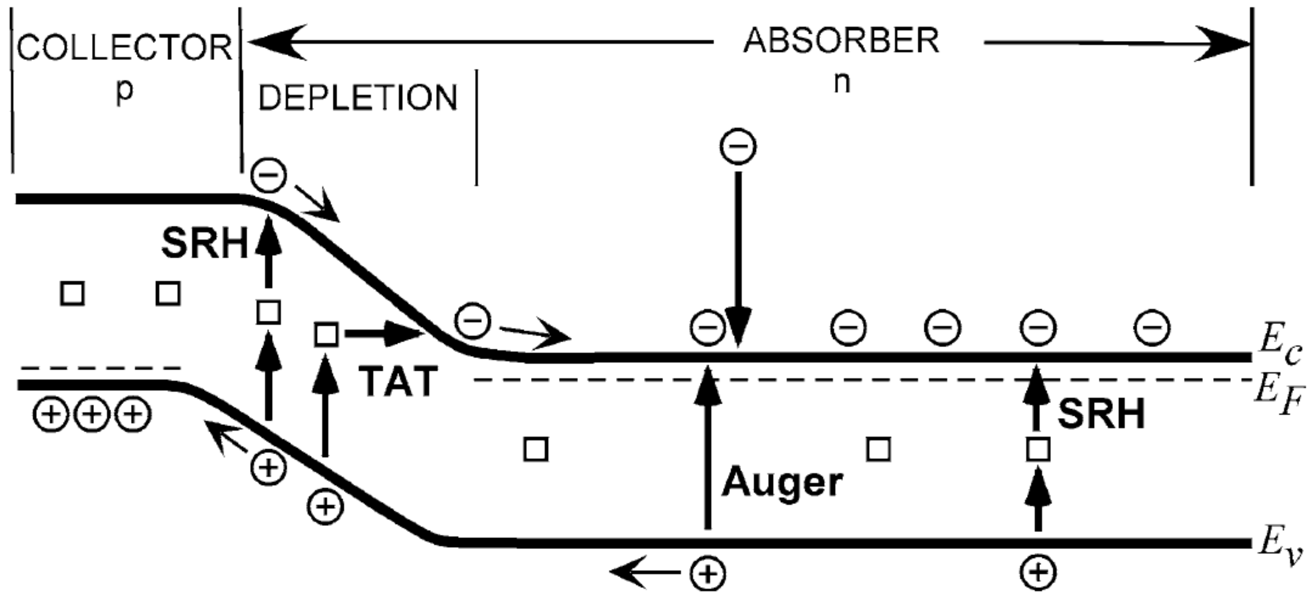

D. R. Rhiger, J. Electronic Materials, 40(8) 1815 (2011)

- High performance IR detector require good signal (photoresponse; QE) to noise (dark current) ratio
  - High QE achieved using thick, strain-balanced absorbers
- Dark current mechanisms in a p-on-n homojunction
  - Trap assisted tunneling, band-to-band tunneling
  - G-R current from SRH processes in depletion region
  - Diffusion dark current from Auger and SRH processes in quasi-neutral region
  - Surface leakage current (not shown)

LWIR Superlattice Properties Deduced from Band Structure (1)

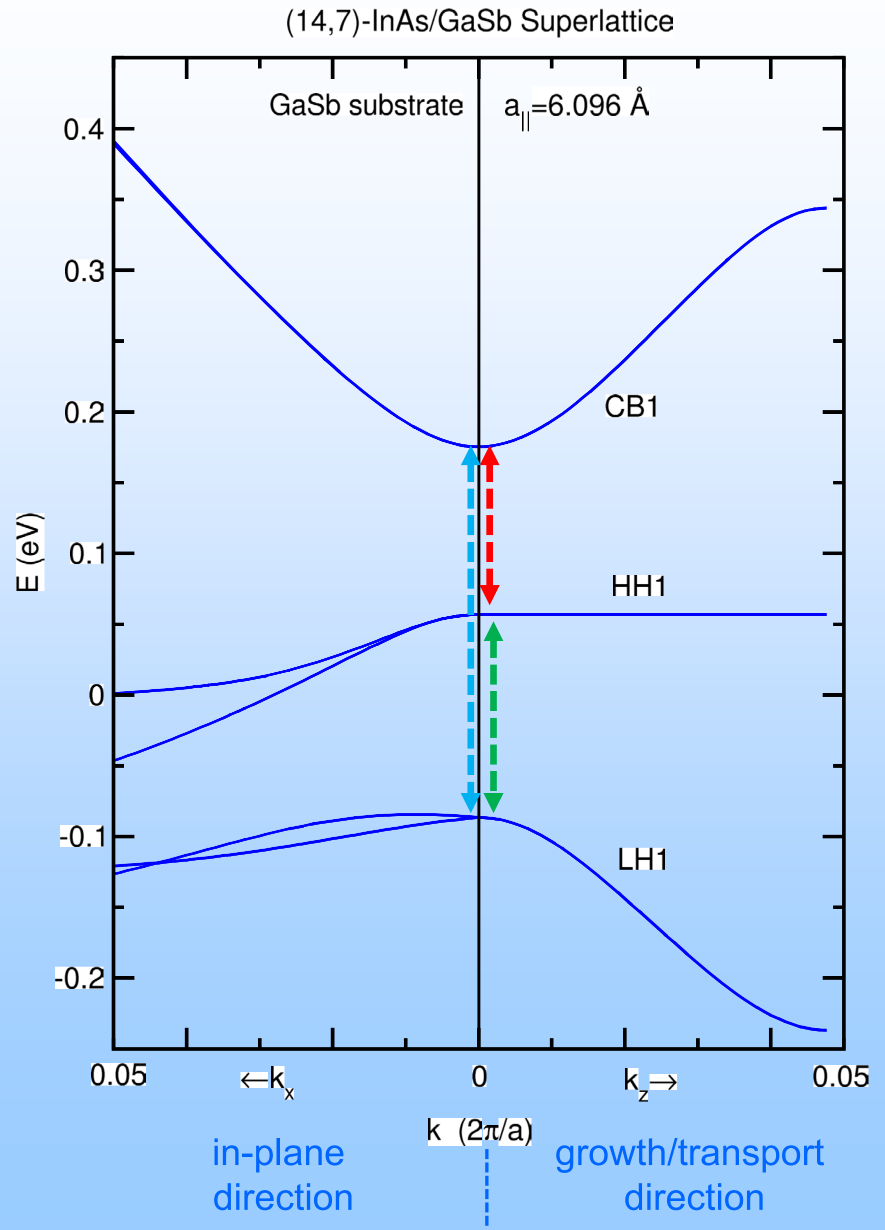

- Key features of LWIR SL band structure
  - Splitting of LH1 and HH1
  - Strong anisotropy in HH1 band
    - Low dispersion along growth/transport direction
- Absorption property
  - Cutoff wavelength determined by $E_g=(E_{c1}-E_{hh1})$
  - Low dispersion in HH1 band along growth direction leads to larger VB edge (2D) density of states for enhanced absorption
    - Compensates for lower oscillator strength
- Reduced electron diffusion current
  - Diffusion current = $eD_e\frac{dn}{dx}$ where $D_e = \frac{\mu_e K_B T}{e}$
  - where $\mu \sim (m^*)^{-3/2}T^{1/2}$ and $m^* = \frac{\hbar^2}{\frac{d^2E}{dK^2}}$
- Reduced tunneling leakage
  - Tunneling current $T(E) = e^{-2\sqrt{\frac{2m^*(V_0-E)(x_2-x_1)}{\hbar^2}}}$
  - where V_0 is potential energy; E is energy; x_1 & x_2 are the positions of the barrier
- Suppressed Auger recombination
  - [$(E_{hh1}-E_{lh1})$ >E_g] favors Auger suppression
  - More easily attained in LWIR than MWIR

Diode Detector vs. nBn Detector

(a) p-n diode

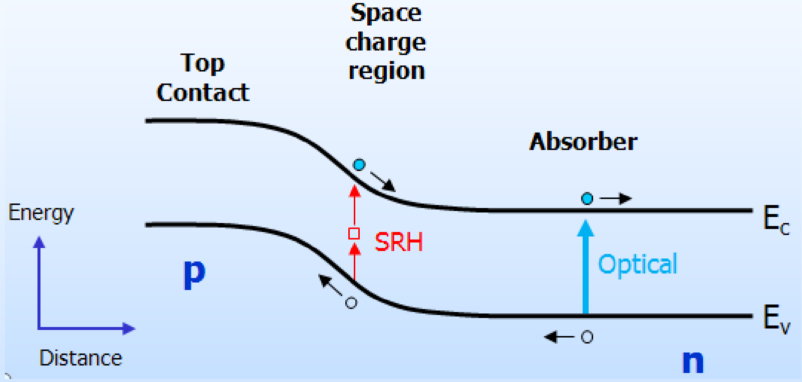

(b) nBn detector

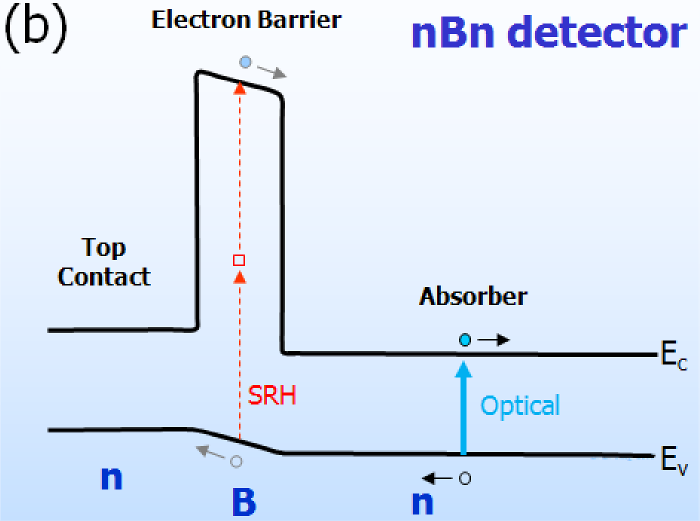

- Conventional p-n junction photodiode
- Suffers from generation-recombination (G-R) dark current
  - Primarily induced by mid-gap defects at the junction via Shockley-Read-Hall (SRH) processes
  - Exponential process with activation energy of $E_g/2$ (half of energy band gap)
- Also suffers from surface leakage dark current
- Resulting high dark current limits sensitivity and/or operating temperature

- Innovative nBn device architecture
  - High band gap electron barrier inserted at the "junction"
  - Blocking electrons but not holes
  - Larger band gap of the barrier suppresses SRH processes and virtually eliminates G-R dark current
  - Barrier also serves to block surface leakage dark current
  - Photocurrent flows un-impeded

Maimon & Wicks, APL (2006)

Developing Extended Cutoff Absorber Material

Material	Growth Mode	λ_{cutoff} Range	Remark
InAs/GaSb T2SL	~ Lattice matched	~2 µm – LWIR	Short lifetime
InAsSb bulk	Lattice matched	4 µm (fixed)	For standard λ_{cutoff} = 4 µm nBn only
InSb QD in InAsSb	Stranski-Krastanov	~6 µm	Bimodal; lower response for λ>4 µm
InSb/InAsSb T2SLS	Strain-balanced	< 5 µm	Limited to thin InSb layers (~3-5 Å)
InSb/InAs T2SLS	Strain-balanced	< 5 µm	Limited to thin InSb layers (~3-5 Å)
InAs/InAsSb T2SLS	Strain-balanced	~4 µm – LWIR	Long lifetime. Easiest to grow.

- Explored many absorber candidates at JPL over a period of two years
- Selected only low-defect growths on GaSb substrate
  - No relaxed metamorphic growth
- Two candidates capable of reaching 5 µm and beyond
  - InAs/GaSb type-II superlattice (T2SL)
  - InAs/InAsSb type-II strained layer superlattice (T2SLS)
- InAs/InAsSb T2SLS has better lifetime and is much easier to grow
  - First successful demonstration of InAs/InAsSb T2SLS nBn in July 2010
  - In 2013, commercial foundry MWIR material reached ~5 µs minority carrier lifetime

InAs/InAsSb SLS
Much Easier to Growth, Much Better Lifetime

Material Growth Shutter Sequence

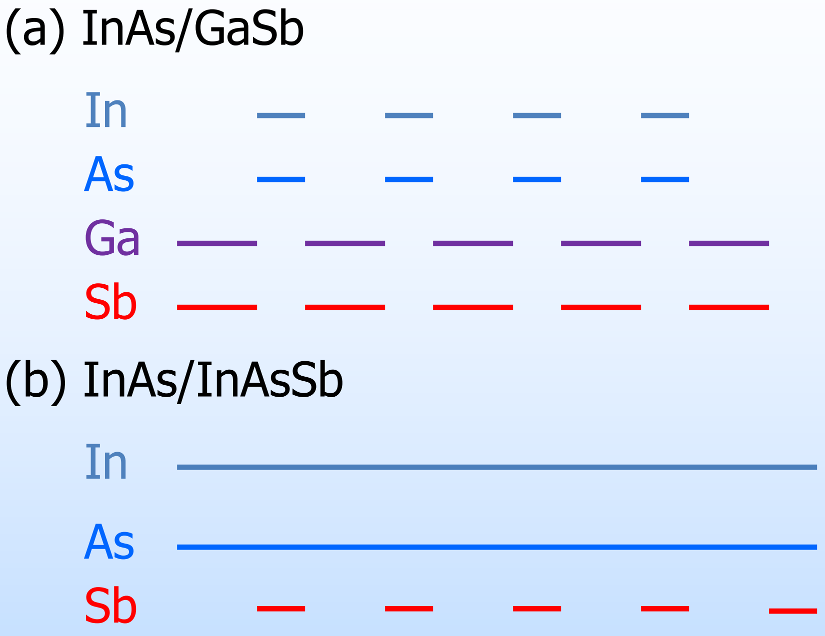

- InAs/InAsSb T2SLS growth is much simpler than InAs/GaSb T2SL
  - 3 elements instead of 4 (no Gallium)
  - 1 moving shutter instead of 4
  - No complicated interface strain balancing
  - The most difficult part is InAsSb (mixed Group V)
  - Cutoff wavelength is easily adjusted
- **Good manufacturability**
- **Much longer minority carrier lifetime** for InAs/InAsSb T2SLS

MWIR InAs/InAsSb T2SLS High Operating Temperature Barrier IR Detector (HOT-BIRD)

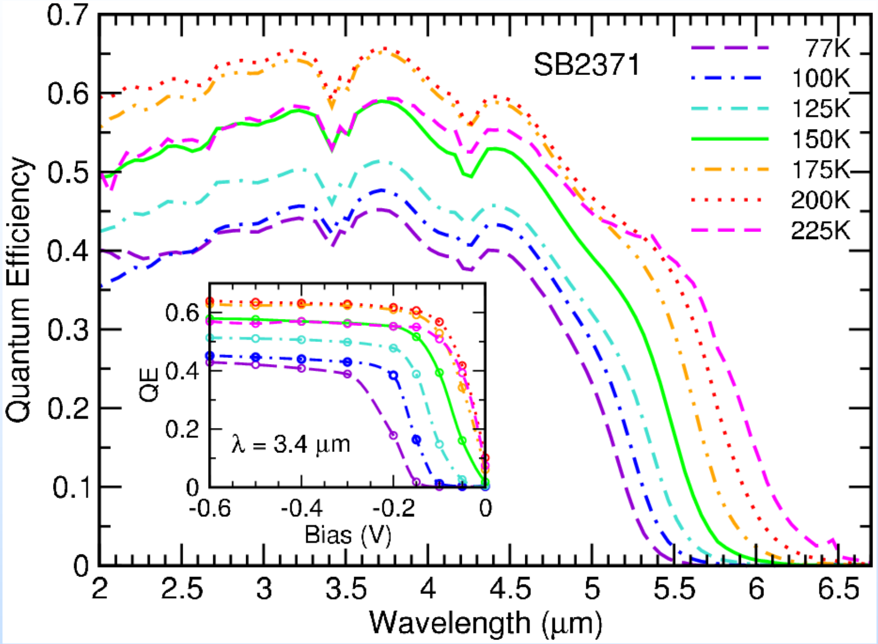

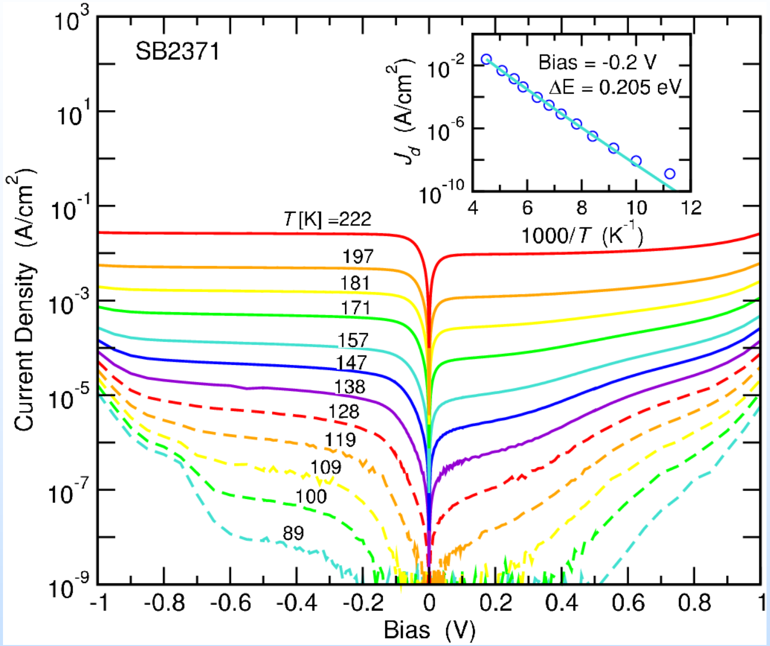

- MWIR nBn detector with InAs/InAsSb T2SLS absorber
- Cutoff wavelength: 5.07 µm (77 K), 5.77 µm (225 K)
- QE(4.3 µm, 150K)=52% – No A/R coating
- J_{dark}(-0.2V, 157K)=9.6×10^{-5} A/cm^2 (~4.5X Rule'07)
- Arrhenius analysis (109 K to 222 K):
  - Activation energy *ΔE* = 0.205 eV ; Eg(157 K) ~0.229 eV.

"**B**arrier **I**nfra**R**ed **D**etectors", D. Z. Ting, A. Khoshakhlagh, A. Soibel, Cory J. Hill, and S. D. Gunapala, U. S. Patent No. 8,217,480 (2012)

Jet Propulsion Laboratory
California Institute of Technology

MWIR HOT-BIRD Successes

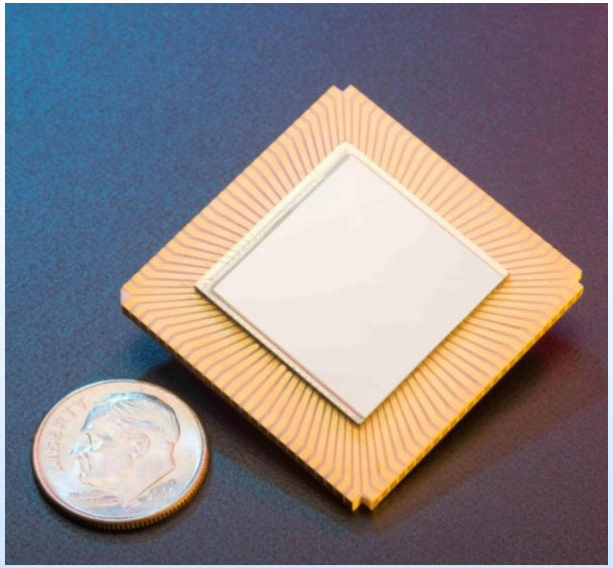

- MW high operating temperature (HOT) barrier infrared detector (BIRD) first demonstrated at JPL in 2010
  - Combines high operating temperature advantages with InSb FPA advantages in uniformity/operability/affordability/large-format capability

MWIR InAs/InAsSb T2SLS HOT-BIRD: NEΔT and Images

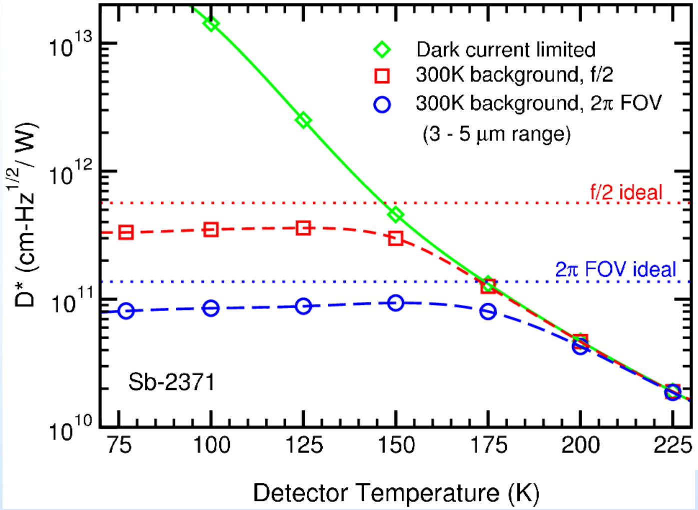

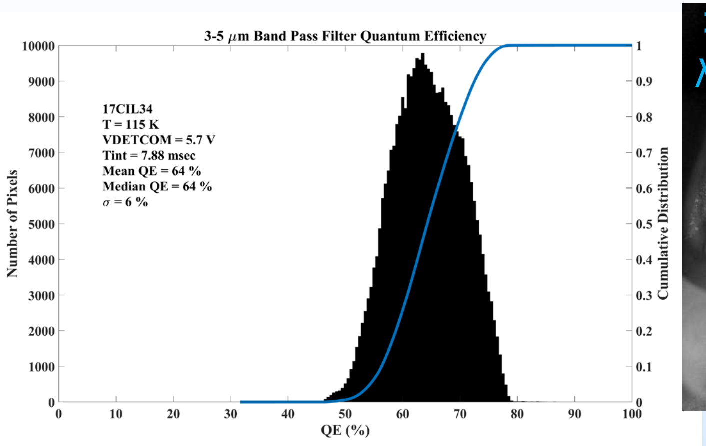

Mean QE 64% without A/R coat

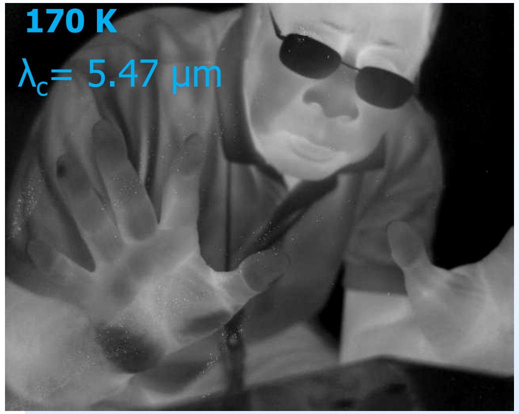

- Black-body (3-5 μm) D*
  - f/2: $D^*=3.4\times10^{11}$ cm-Hz$^{1/2}$/W, BLIP at 152 K
    - Assuming J_{dark} = ¼ J_{photo}
- FPA shows **significantly higher operating temperature than InSb**
  - SBF-193 ROIC: 24-μm pitch, 640×512 format
  - f/2 optics, 300K background
  - 160K: NEDT 18.7 mK, Operability 99.7%
  - 170K: NEDT 26.6 mK, Operability 99.6%

HOT-BIRD: "Mid-wavelength **h**igh **o**perating **t**emperature **b**arrier **i**nfra**r**ed **d**etector and focal plane array", D. Z. Ting, A. Soibel, A. Khoshakhlagh, S. B. Rafol, S. A. Keo, L. Höglund, A. M. Fisher, E. M. Luong, and S. D. Gunapala, *Appl. Phys. Lett.* **113** , 021101 (2018). doi: 10.1063/1.5033338

LWIR T2SLS Detectors & FPAs

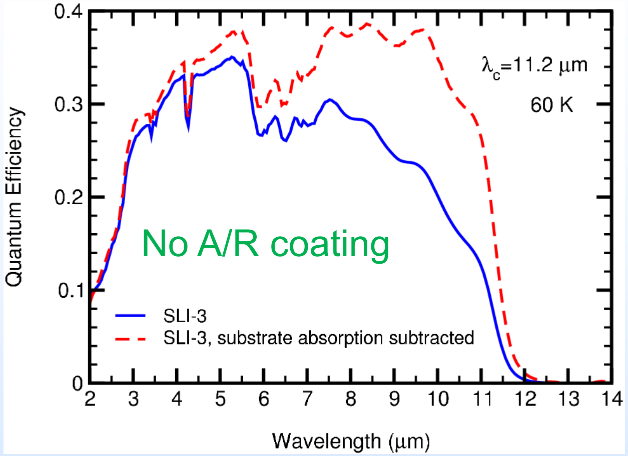

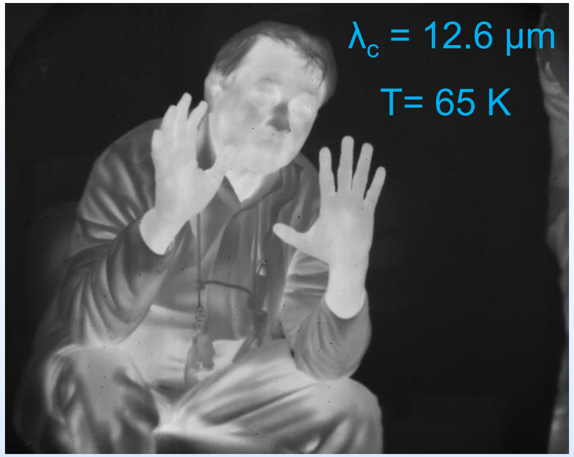

99.98% operability (18SLL03)

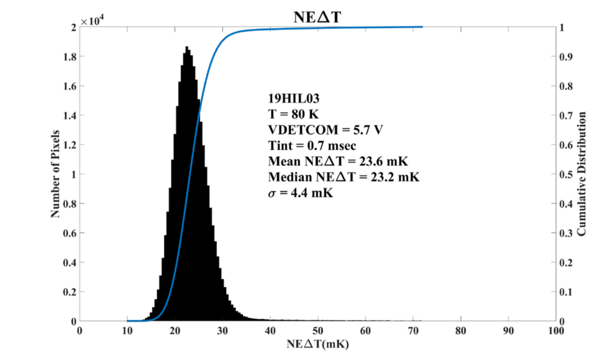

NEΔT of 11μm Hyperspectral Thermal Imager (HyTI) FPA @80K

- Developing T2SL-based LWIR detectors for NASA Sustainable Land Imaging Technology (SLI-T) Program
- Unipolar barrier infrared detector architecture, T2SL absorber
  - High quality λ_{cutoff} ~ 11.2 μm T2SL absorber material
  - 240 ns minority carrier lifetime
  - $J_{dark}(60K) \sim 10^{-5}$ A/cm^2 ; QE ~ 37% without A/R coating
- Also demonstrated λ_{cutoff} ~ 13.5 μm detectors/FPAs

LWIR-BIRD: David Z. Ting, Alexander Soibel, Arezou Khoshakhlagh, Sam A. Keo, Anita M. Fisher, Sir B. Rafol, Linda Höglund, Cory J. Hill, Brian J. Pepper, and Sarath D. Gunapala "Long wavelength InAs/InAsSb superlattice barrier infrared detectors with p-type absorber quantum efficiency enhancement", Appl. Phys. Lett. 118, 133503 (2021); https://doi.org/10.1063/5.0047937

Initial HOT-BIRD Performance

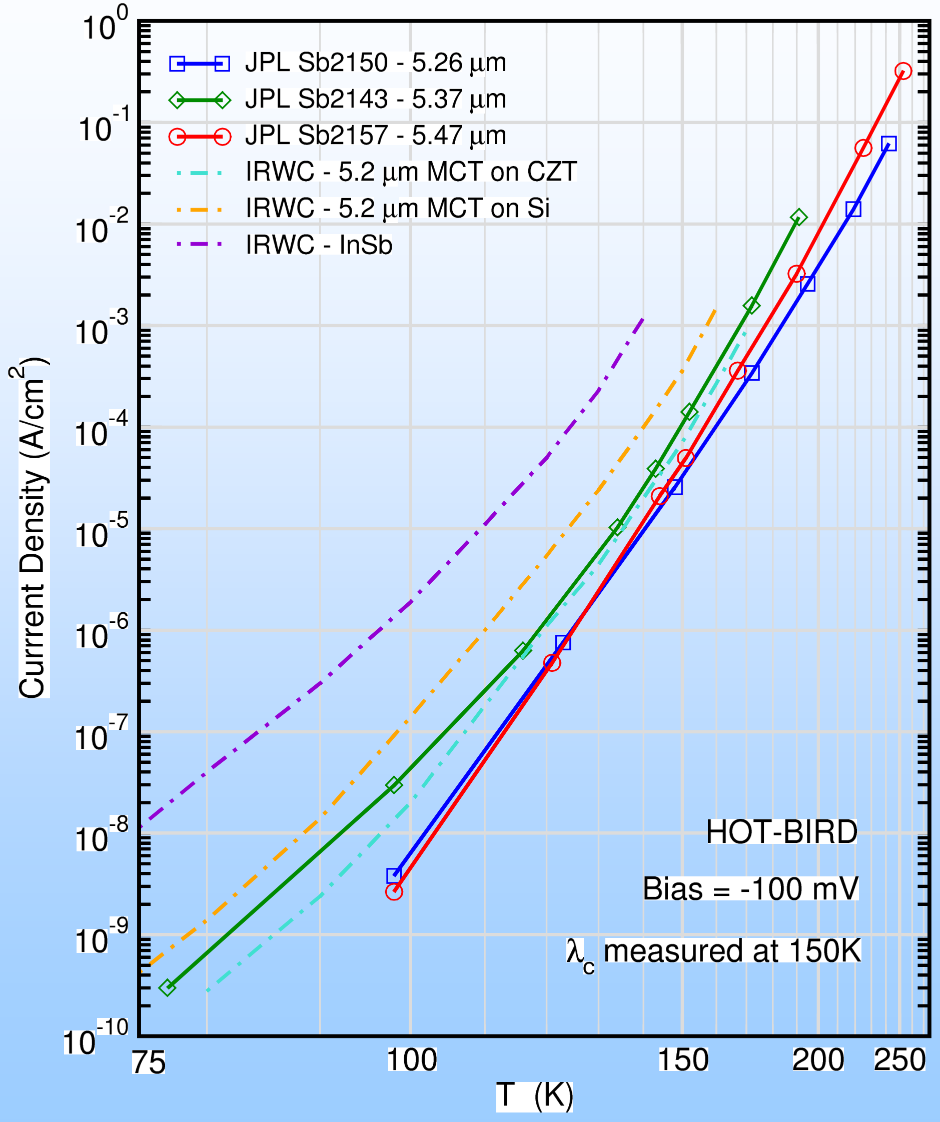

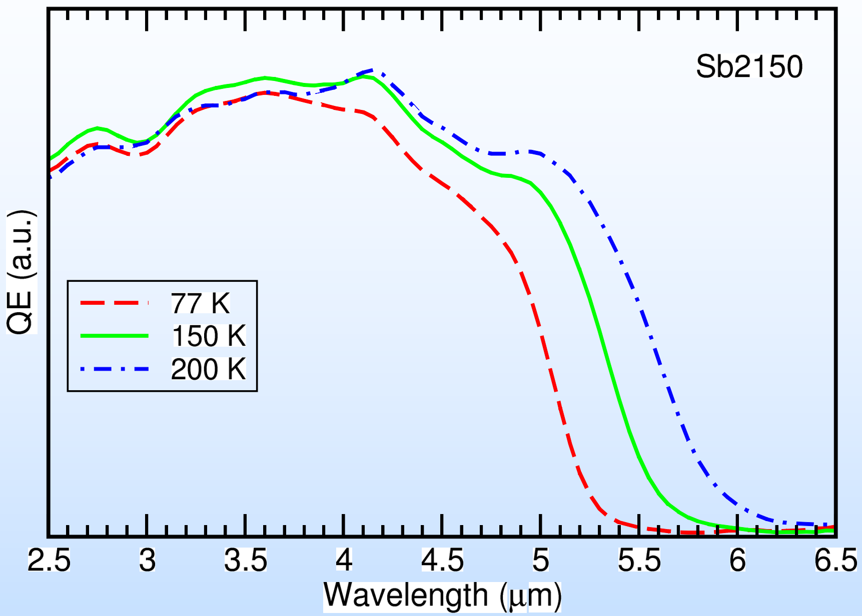

- λ_c >5 µm achieved in July 2010
- Dark current performance comparable to MCT on CZT from RVS Infrared Wall Chart (IRWC)
  - Better than InSb, MCT-on-Si
- Combines the advantages of InSb and MCT

T2SLS Barrier IR Detector (BIRD) Benefits

- Superlattice benefits
  - Continuous cutoff wavelength adjustability
    - InAs/GaSb: NIR to VLWIR. InSb/InAsSb: MWIR. InAs/InAsSb: MWIR to VLWIR.
  - Auger suppression
  - Tunneling reduction
- Ga-free superlattice (InAs/InAsSb) benefit
  - Lot easier to grow than InAs/GaSb T2SL
  - InAs/InAsSb T2SL is more defect tolerant than InAs/GaSb T2SL
- nBn benefits
  - Suppresses SRH (G-R) dark current
  - Photocurrent flows un-impeded/ resulting in higher operating temp.
- III-V semiconductor benefits
  - Less ionic; stiffer. Robustness for manufacturing
  - Substrates are readily available and affordable
  - Large area GaSb substrates for the antimonides (4”,5”, & 6”)

T2SLS FPA for Space Science Applications

Hyperspectral Thermal Emission Spectrometer (HyTES)

The Hyperspectral Thermal Emission Spectrometer (HyTES) is an airborne imaging spectrometer with 256 spectral channels between 7.5 and 12 micrometers in the thermal infrared part of the electromagnetic spectrum and 512 pixels cross-track. HyTES is being developed to support the Hyperspectral Infrared Imager (HyspIRI) mission. HyspIRI includes two instruments mounted on a satellite in Low Earth Orbit. There is an imaging spectrometer measuring from the visible to short wave infrared (VSWIR) and a multispectral thermal infrared (TIR) imager.

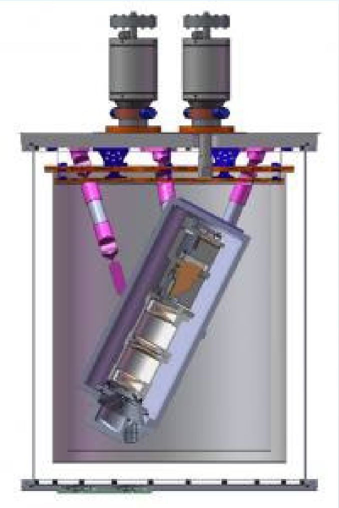

HyTES

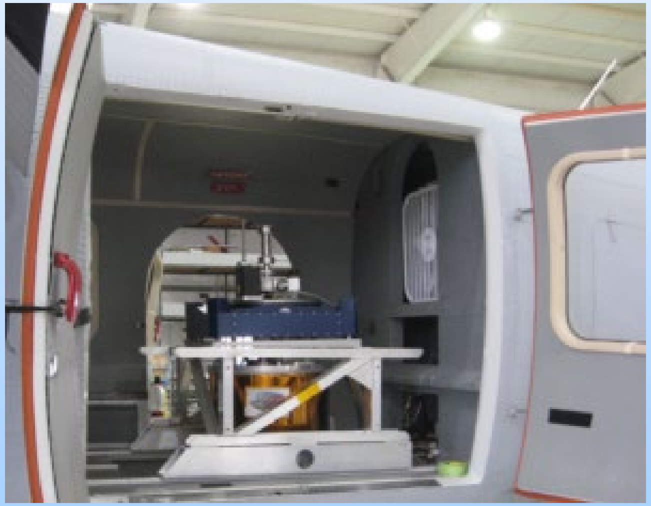

HyTES on Twin Otter

HyTES on ER-2 Aircraft

Reference: https://hytes.jpl.nasa.gov/

HyTES Performance with T2SL FPA

BIRD installation and verification in HyTES

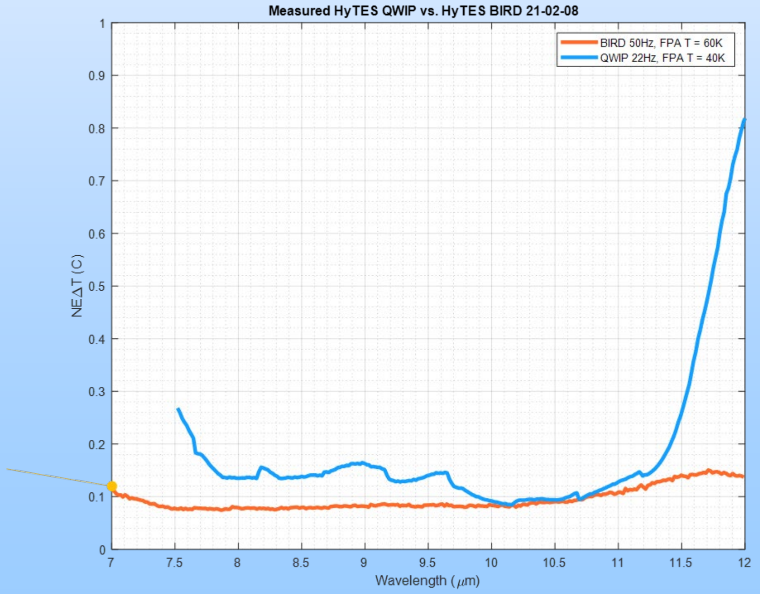

Reference: https://hytes.jpl.nasa.gov/

L1 Brightness Temperature

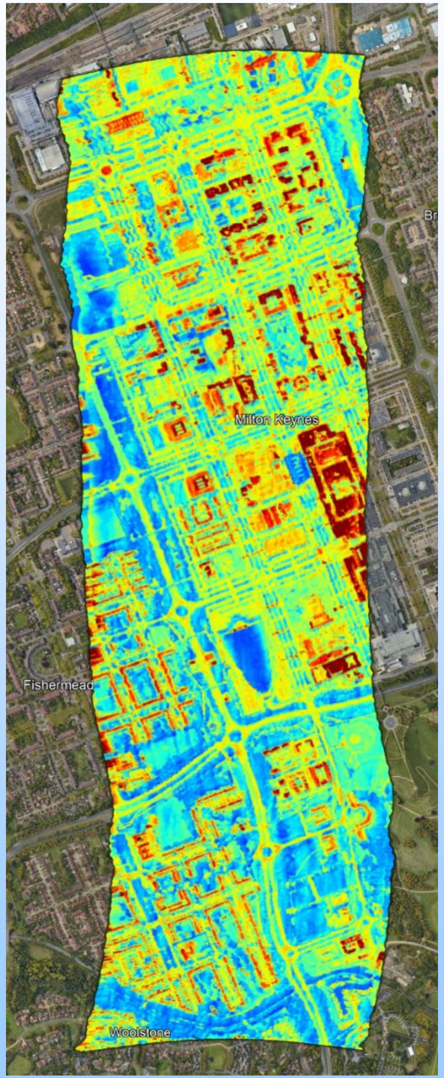

L2 Land Surface Temperature

Hyperspectral Thermal Imager (HyTI)

HyTI Instrument & FPA Performance Data

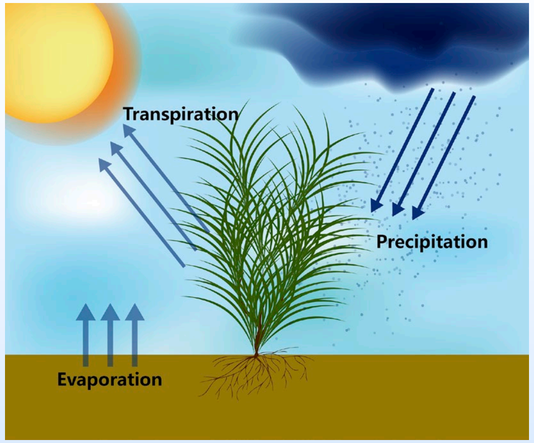

Evapotranpiration

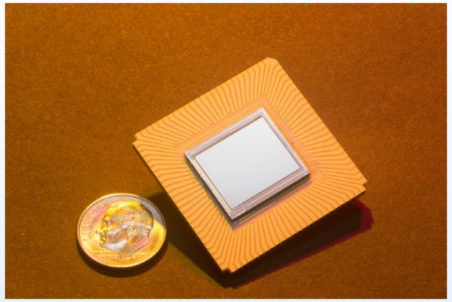

HyTI T2SL LWIR
Focal Plane Array

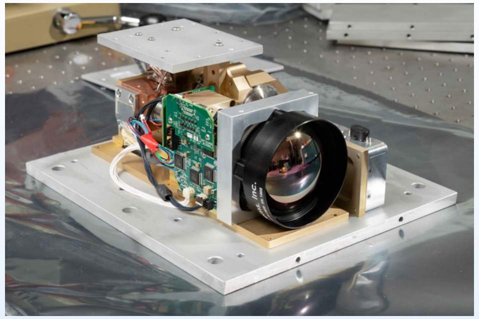

HyTI Instrument (~2U)

Artist rendering of HyTI Spacecraft
(Scheduled for April 4, 2024 launch)

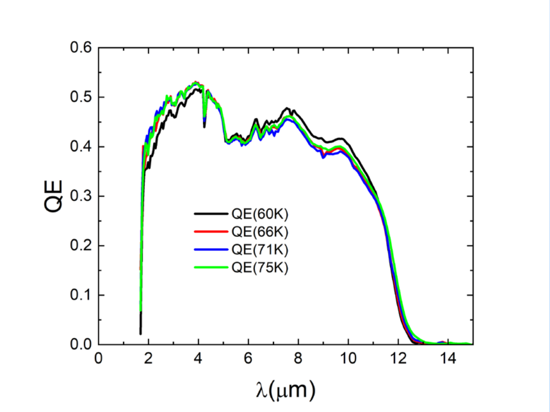

Quantum Efficiency
Spectrum

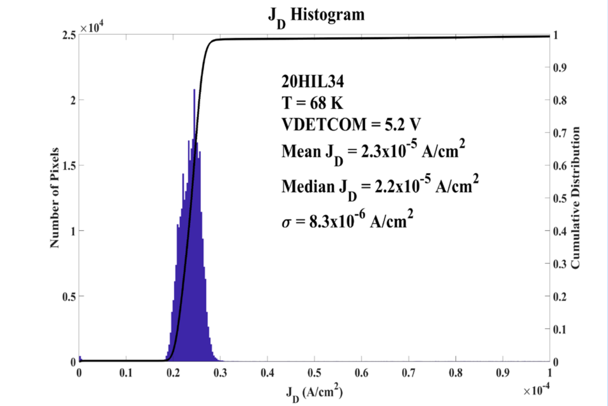

J_D Histogram

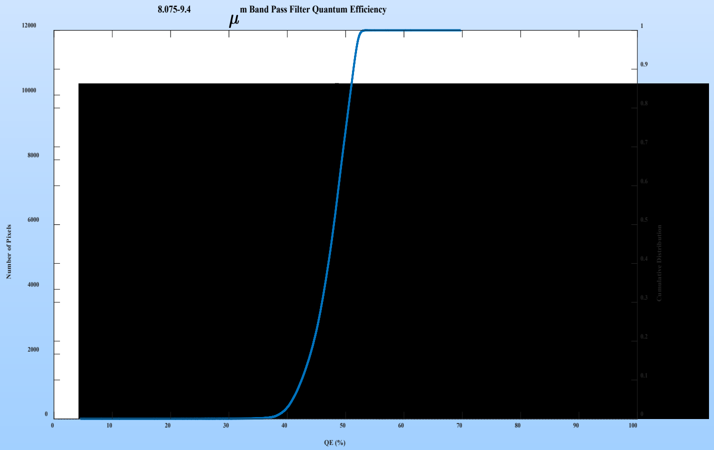

Mean QE ~48%

1/f Noise of HyTI FPAs

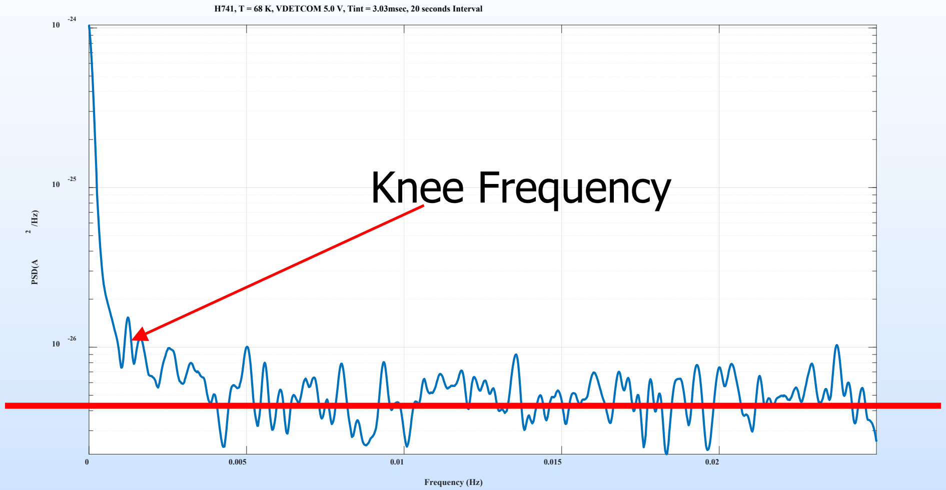

Detector bias – 0V
Knee frequency ~1mHz

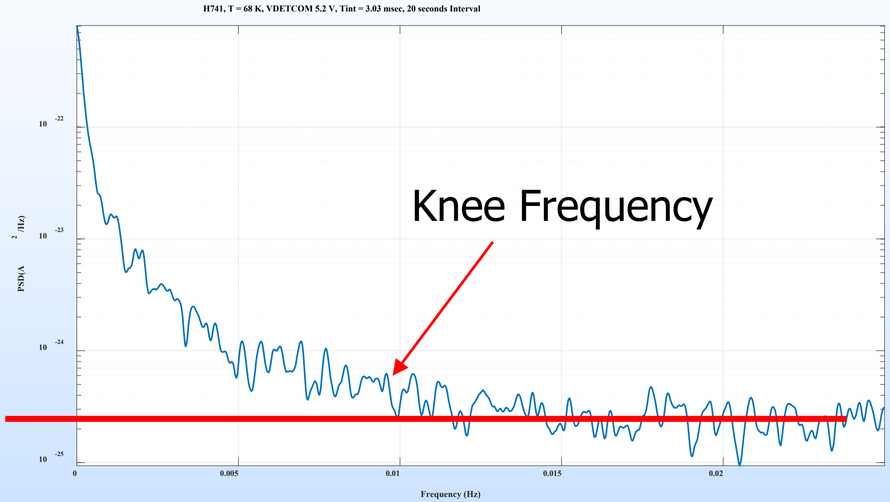

Detector bias – 100mV
Knee frequency ~10mHz

Sun Rise Seen from ISS

Wild Fire & Volcanic Eruption

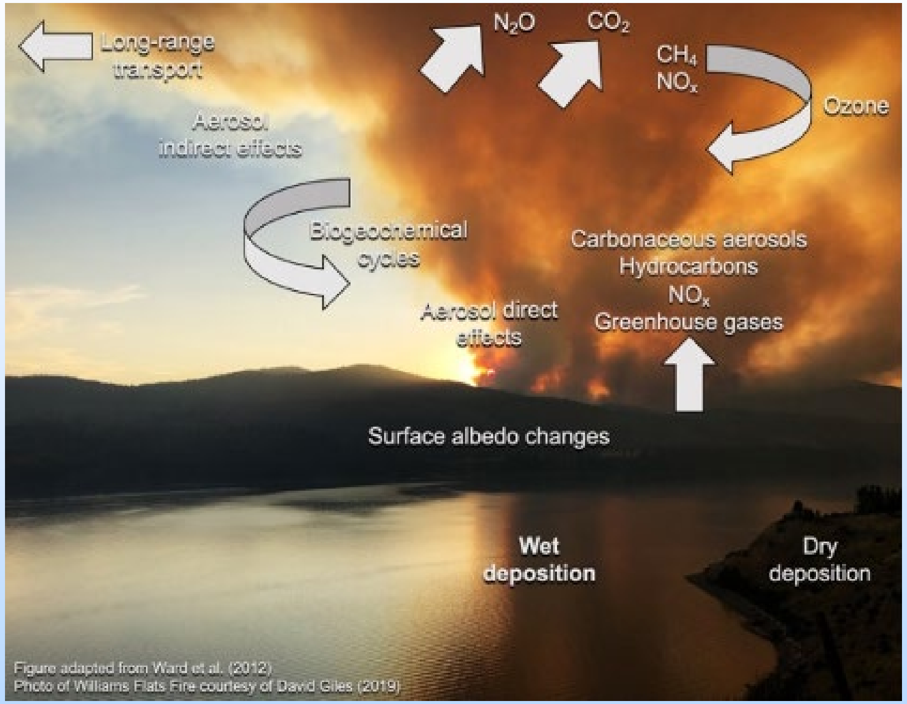

The Dixie Fire was an enormous wildfire in California in 2021. It burned 963,309 acres before being 100% contained after 4 months. It was the largest single wildfire in recorded US history, and the second-largest wildfire overall. This fire completely destroyed several small towns, burning an area larger than the state of Rhode Island. Smoke from the Dixie Fire caused unhealthy air quality across the Western United States, including states as far east as Utah and Colorado. The Dixie Fire was the most expensive wildfire fought in the United States history, costed ~$640M.

Hot Target Detection Requirements (Cont.)

- Instruments on polar-orbiting platforms provide some additional wavelengths, but there are issues with saturation of the MWIR bands for extremely hot targets.

Flaming fire as seen with a visible camera

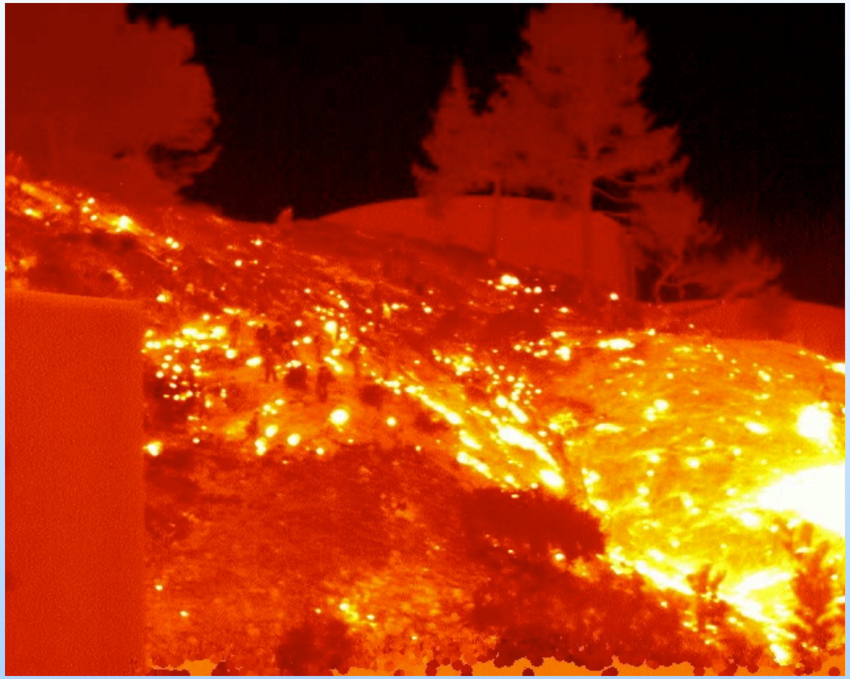

Fire behind JPL in 2011 as seen with a MWIR T2SLS camera

Volcanic Eruptions on Io

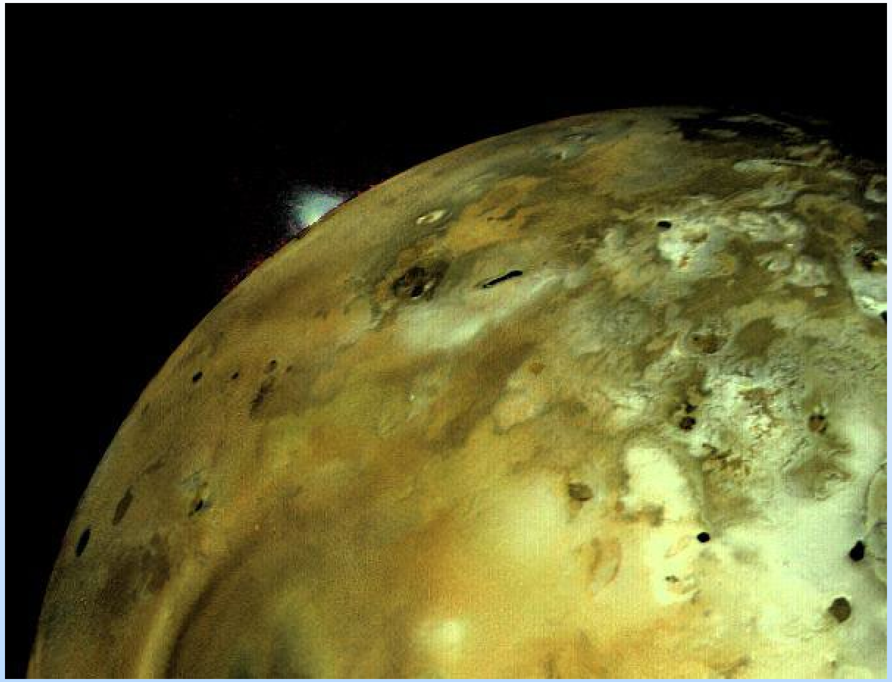

Volcanic eruption of Gallian moon Io as seen in visible by NASA/JPL Voyager 1 spacecraft in 1979

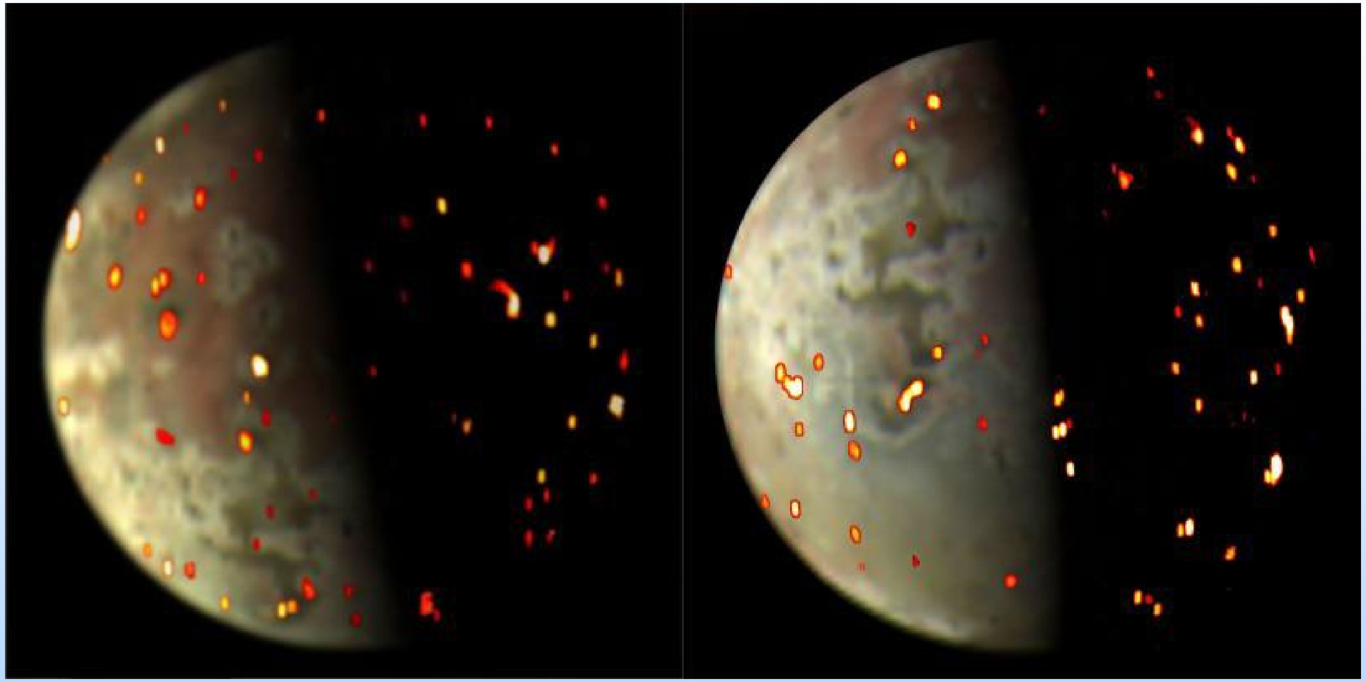

Composite images of Io from the Juno spacecraft at visible (JunoCAM) and infrared (JIRAM) wavelengths, the latter showing thermal emission at 4.8 μm from sites of ongoing volcanic eruptions.

Credit: NASA/JPL-Caltech/SwRI/ASI/INAF/JIRAM. PIA25888.

Digital Read Out Integrated Circuits (DROICs)

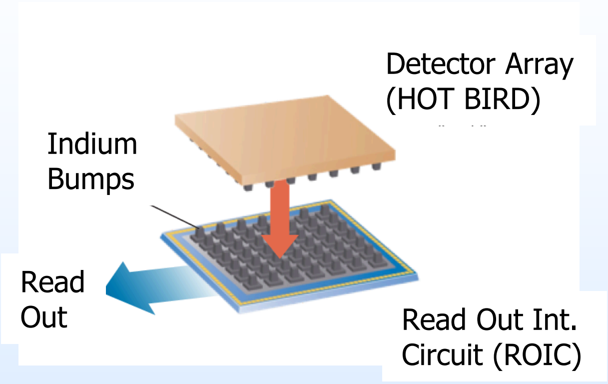

Analog ROIC

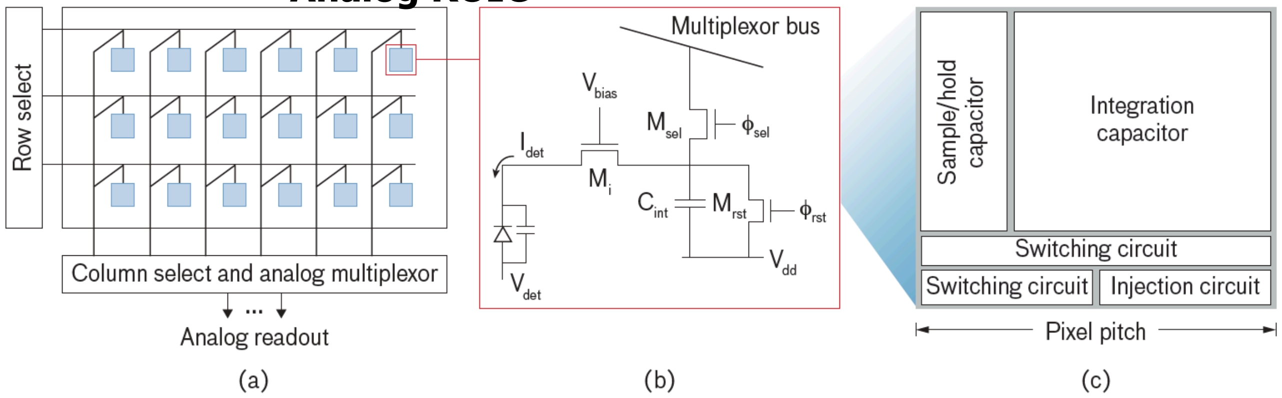

Digital ROIC

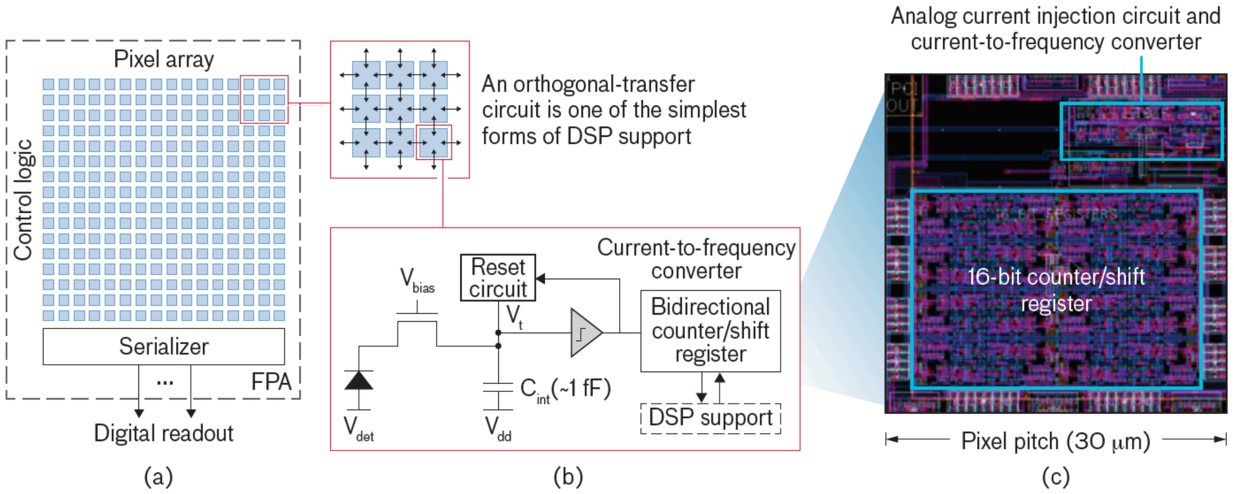

1. "Design and Testing of an All-Digital Readout Integrated Circuit for Infrared Focal Plane Arrays", M. W. Kelly, et al., Proc. SPIE, 5902, (2005).
2. "A new digital readout integrated circuit (DROIC) with pixel parallel A/D conversion and reduced quantization noise", Hüseyin Kayahan ⇑, Melik Yazici, mer Ceylan, and Yasar Gurbuz, Infrared Physics & Technology 63 (2014) 125–132, http://dx.doi.org/10.1016/j.infrared.2013.12.013

Digital HOT-MWIR Imagery

Digital ROIC. λ_{cutoff} (150K) ~ 4.3 μm

t_{integ} ~ 10 ms

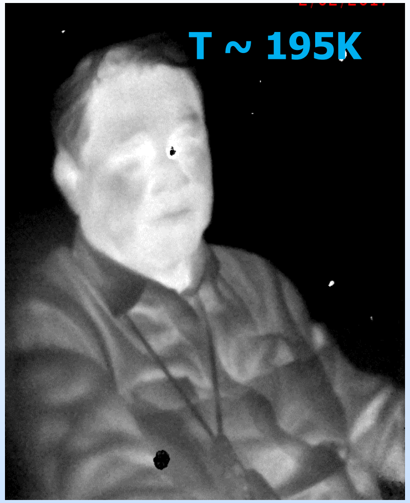

t_{integ} ~ 5 ms

t_{integ} ~ 2 ms

- Encouraging initial 200K imaging results.
- Work in progress
- Un-optimized FPA operating conditions
- Long integration times (better S/N) at 200K made possible by DROIC
  - Two-point correction not possible w/ analog ROIC

Analog ROIC. λ_{cutoff} (150K) ~ 5.8 μm

t_{integ} ~ 6.7 ms

t_{integ} ~ 0.14 ms

- Comparison to FPA w/ conventional analog ROIC
  - Longer cutoff material designed for other applications. Higher dark current at high T.
- Much shorter integrations times at higher T
  - 130K, 6.7 ms intg time, 2-point correction
  - 184K, 0.14 ms intg time, 1-point correction
    - Image would improve with DROIC

Current Remote Sensing Wildfires

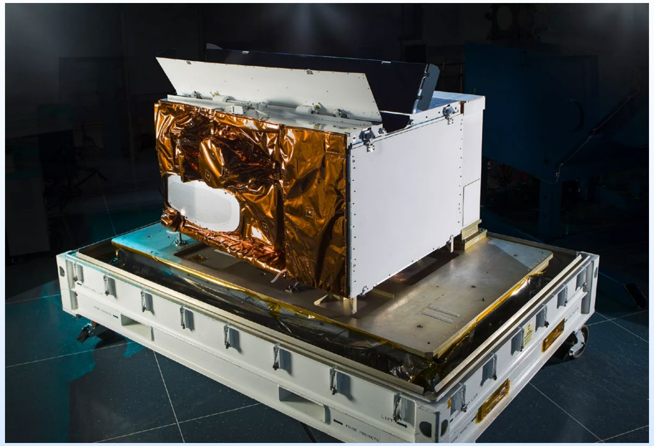

Visible Infrared Imaging Radiometer Suite (VIIRS)
Source: NOAA

Swath width - 3060km
Orbit – Polar at altitude of 829km
Spatial resolution (GSD) – 750m
Spectral bands – 22 (Vis, MWIR, LWIR)
Power – 200W
Weight – 275Kg
Global coverage – 14 Hours
Repeat cycle – 16 days

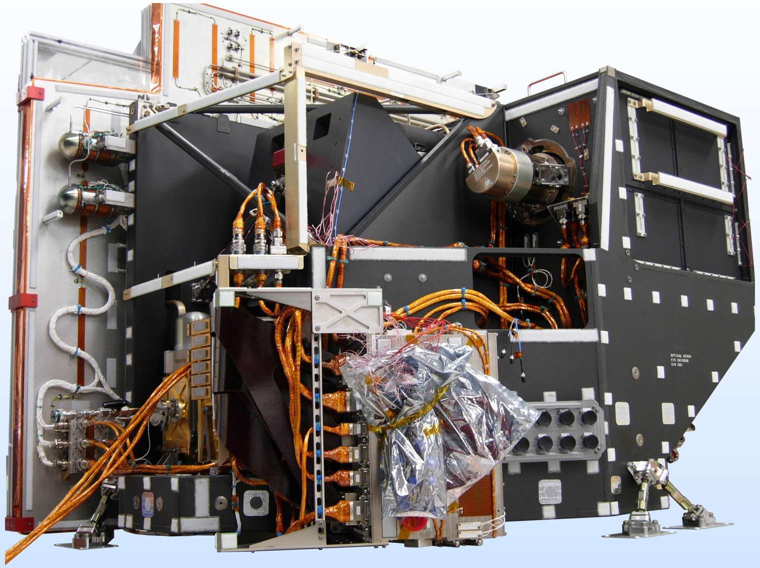

GOES-R Advanced Baseline Imager (ABI)
Source: NASA/NOAA

Orbit – Geo stationary
Spatial resolution (GSD) – 1Km & 2Km
Spectral bands – 16 (Vis, MWIR, LWIR)
Continental US coverage – 5 Min
Hemisphere coverage – 15 minutes

Hot Target Detection Requirements

Jet Propulsion Laboratory
California Institute of Technology

- Due to the wide range of scales involved, understanding the diverse effects of fires and volcanoes in the Earth system requires routine global monitoring only possible from satellites.
- The physics of the retrieval of thermal energetics for these types of hot targets requires sensitivity at multiple wavelengths in the SWIR to MWIR to allow fitting to the Planck blackbody emission curve.
- According to the 2017-2027 National Academies Earth Science Decadal Survey, for target identification and geolocation, fine spatial resolution (30 – 60 m) is required, due to the presence of materials at different temperatures within the area of a single image pixel.
- Currently, no instrument is able to span the entire dynamic range of fires that are present in the Earth system, leading to biases in our understanding of the fire occurrence frequency on the ends of the size/temperature spectrum.

Artist rendering of a fire detection satellite on orbit

Jet Propulsion Laboratory
California Institute of Technology

Compact Fire Infrared Radiance Spectral Tracker (c-FIRST)

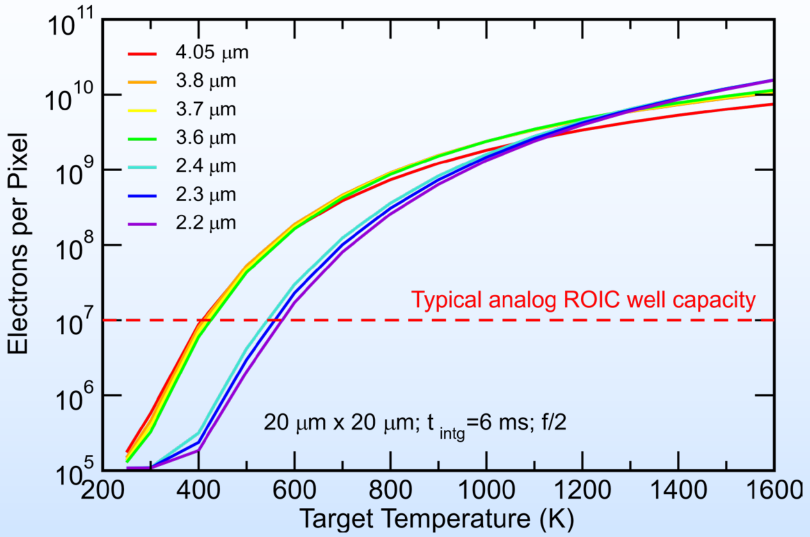

Digital-FPA Performance on HOT Targets

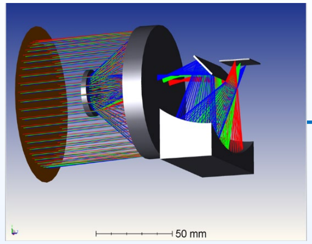

Off-Axis All Metal Korsch Optical Design

c-FIRST Instrument

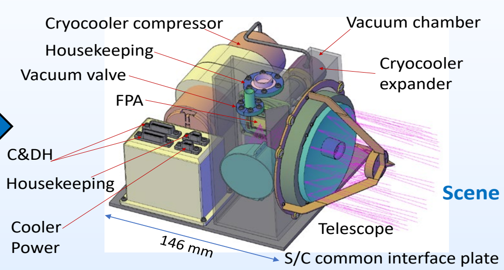

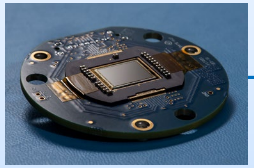

High Dynamic Range Digital FPA

Qualcomm Snapdragon 855 board

Science and Societal benefits

- Detect small fires with good geolocation and large fires without saturating the instrument
- Quantify the flow of carbon in terrestrial ecosystems.
- Discover cascading perturbations in ecosystems related to carbon storage.
- Understand ecosystem response to fire events.
- Understand how the threat of wildfires is changing with time and how exposure to emissions from wildfires can affect human health.

c-FIRST Instrument

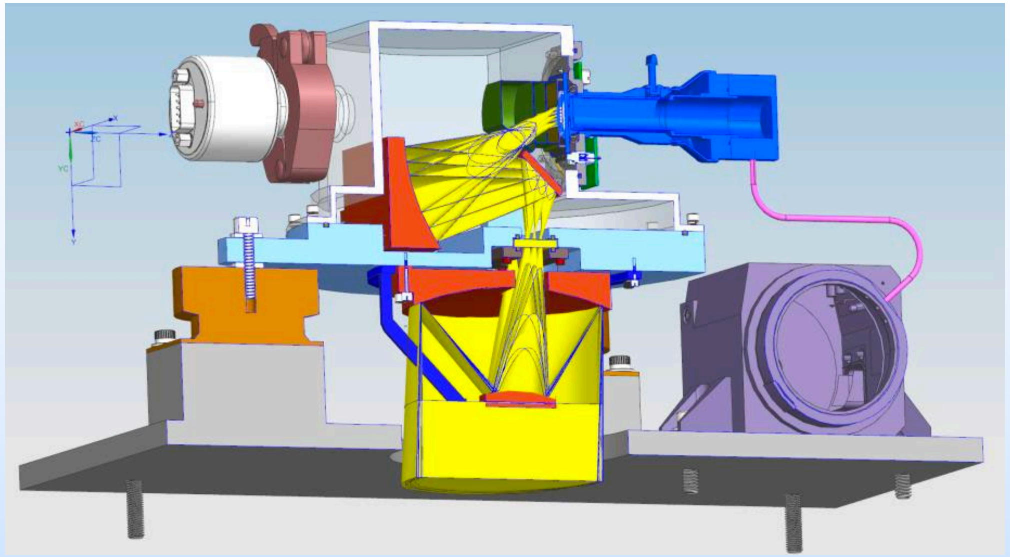

Cross Section of Updated c-FIRST Engineering Model Source: NASA/JPL

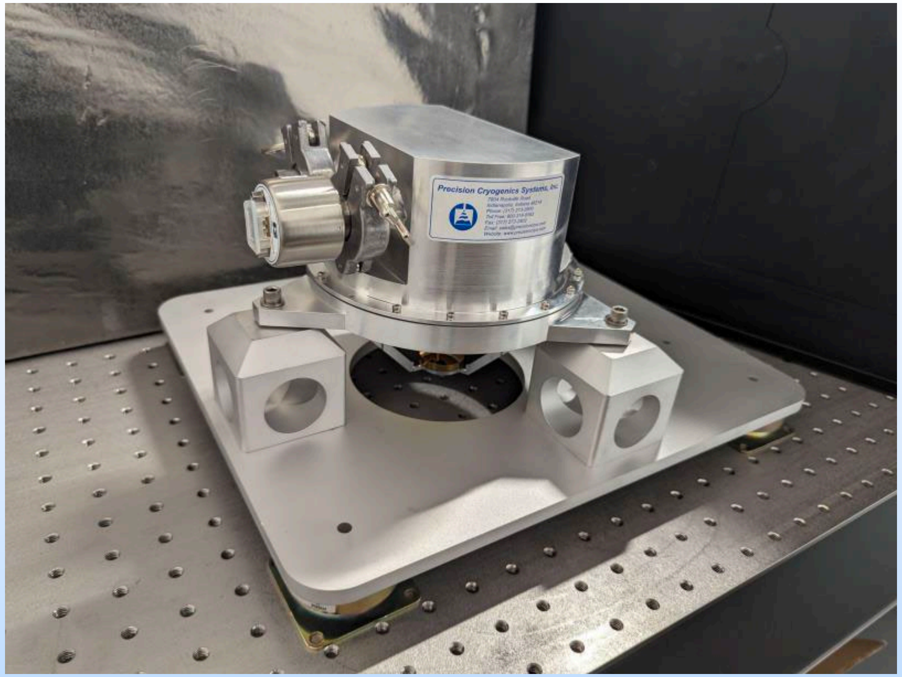

- 4 mirrors
- Path of light in yellow

Weight	- 7 Kg
Power	- 40W
FPA	- 1280x480 T2SLS
Pixel	- 20μm
Aperture	- 80mm
GSD	- 50m
Detectable Temp.	- 300 to >1600K
Cross track	- 64Km
Spectral bands	- 5
FPA operating Temp.	- 150K
Frame rate	- 150Hz
NEDT	- <0.7K
FOV	- 7.3 degrees

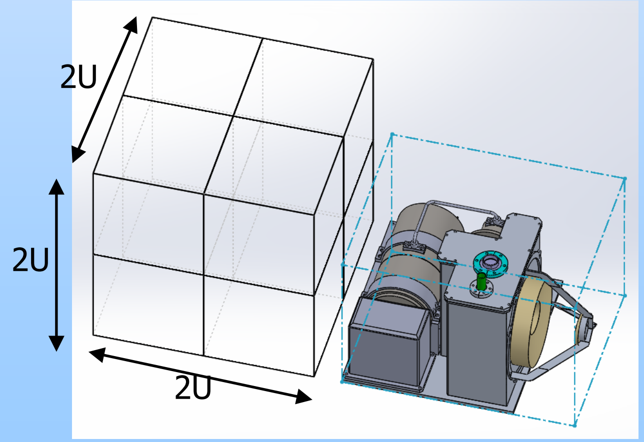

Jet Propulsion Laboratory
California Institute of Technology

PIRS for Fire Science

Proposed Goals

We aim at answering the following science questions:

- How do 3-D boundary layer structures interact with wildfire (e.g., pyroCb) initiation and development?
- How do 3-D moisture transport interact with wildfire (e.g., pyroCb) initiation and development?
- How do high-resolution 3-D meteorological conditions (e.g., soundings of T and q profiles) help improve model prediction of fire weather?

Why Hyperspectral Sounder CIRAS

- High-resolution Imagers like MODIS and VIIRS can provide 2-D surface meteorological data (e.g., surface T) at high spatial resolution (e.g., 1-km FOV). But they do not provide T and q (specific humidity) vertical profiles.
- Profiles of T and q inform us additional information that is essential in forecasting for fire weather condition and fire behavior development.
- For example: Boundary layer stability, and upper level dry air intrusion to the surface, or moist air that helps development of pyroCb from pyroCu.

Example of Fire Behavior and Boundary Layer Stability

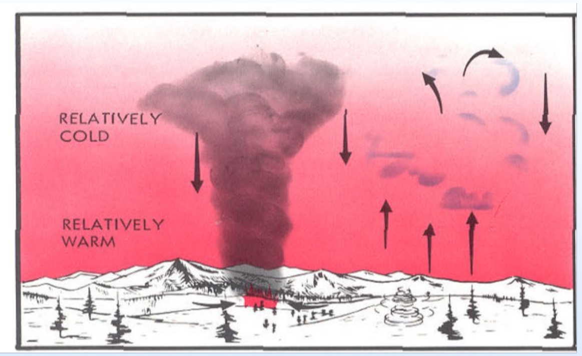

Warm below, cold above: Unstable boundary layer, high mixing level. Encourage pyro-convection and help burning efficiency because of good ventilation

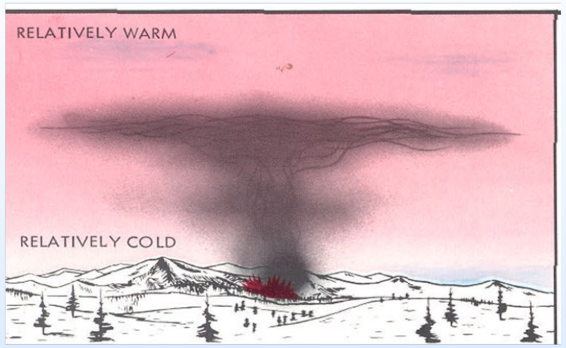

Cold below, warm above: Stable boundary layer, inversion layer capped any vertical transport. Horizontal spread of smoke, bad air quality

CIRAS Band Provides Good T, q Sounding Information in the Lower Troposphere

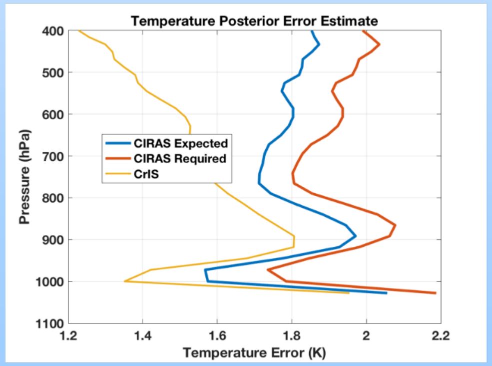

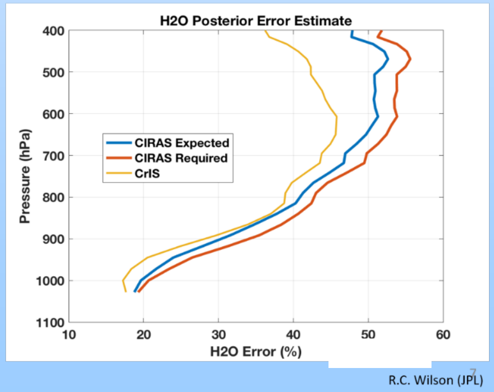

R. C. Wilson (JPL)

Applications in Sustainable Land Imaging

Case Study: Digital BIRD FPA for Land Imaging to Meet New Challenges (Imager)

ROIC	ISC-9803 AROIC	ISC-0905 AROIC	Copious DROIC
Binning	1 × 1	1 × 1	1 × 1
ROIC Format	640 × 512	640 × 512	640x480
Pixel Pitch	25 µm	30 µm	20 µm
Well Depth	11 Me^-	18 Me^-	230 Me^-

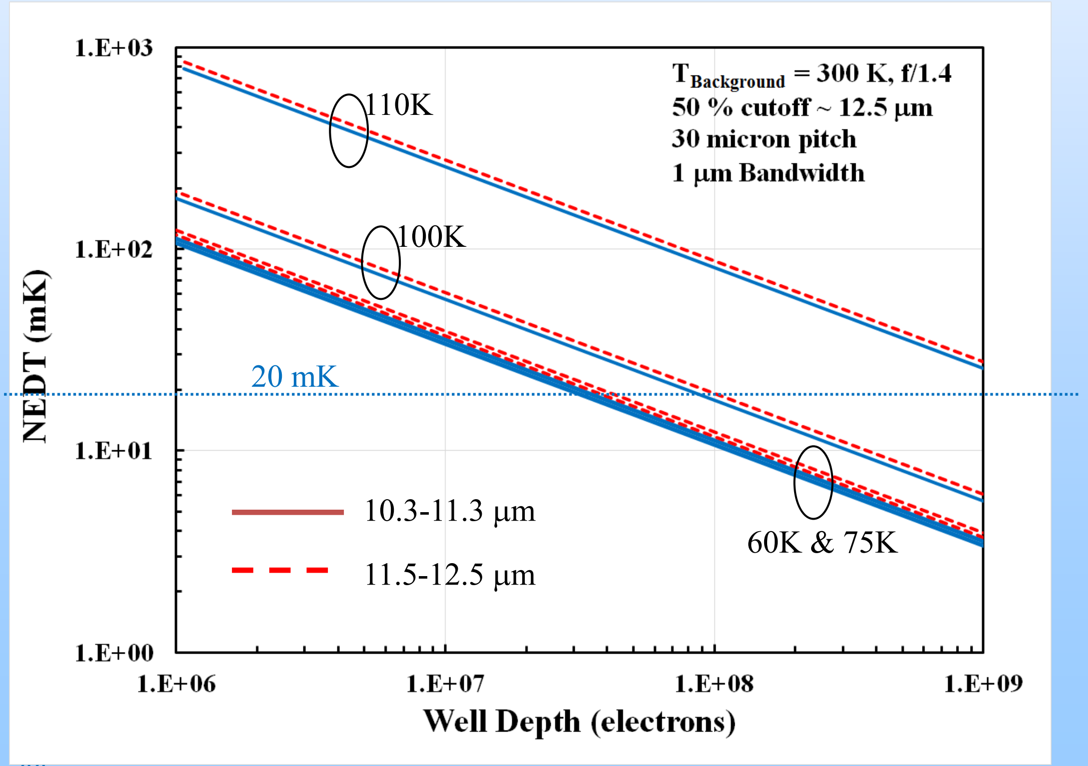

- Addressing challenges with Digital BIRD FPA
  - BIRD for improved detector dark current and QE performance over QWIP
  - Digital-pixel ROIC with large well depth enables much longer integration time to improve signal to noise ratio
    - Conventional ROIC well depth ~ few million e^-'s
    - D-ROIC well depth can exceed 1 billion e^-'s
  - Can achieve 20 mK NEDT for 500 nm wide spectral band centered at 5 – 12.5 µm only with D-ROIC large well depth

NASA SmallSat Fleet

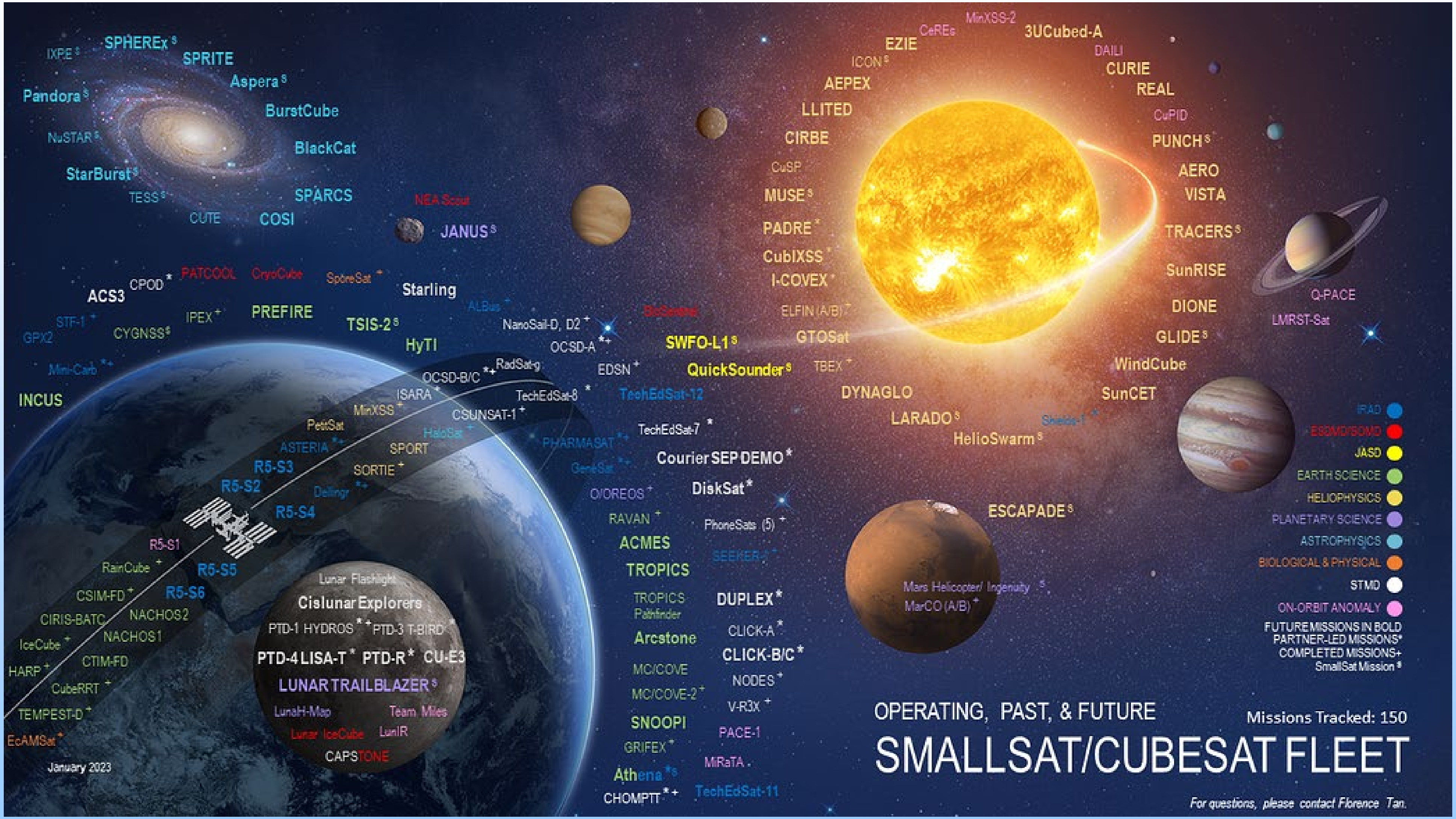

Commercial T2SL Cameras – Civilian Applications

FLIR A6750 SLS

FLIR A6780 SLS

FLIR A8580 SLS

FLIR X6980 SLS

FLIR X8580 SLS

FLIR Neutrino IS HOT MWIR Series

FLIR Neutrino SWaP HOT MWIR Series

Reference: https://www.flir.com/browse/rampd-and-science/high-performance-cameras/

FLIR licensed 12 JPL T2SL patents through Caltech

T2SL for Defense Applications

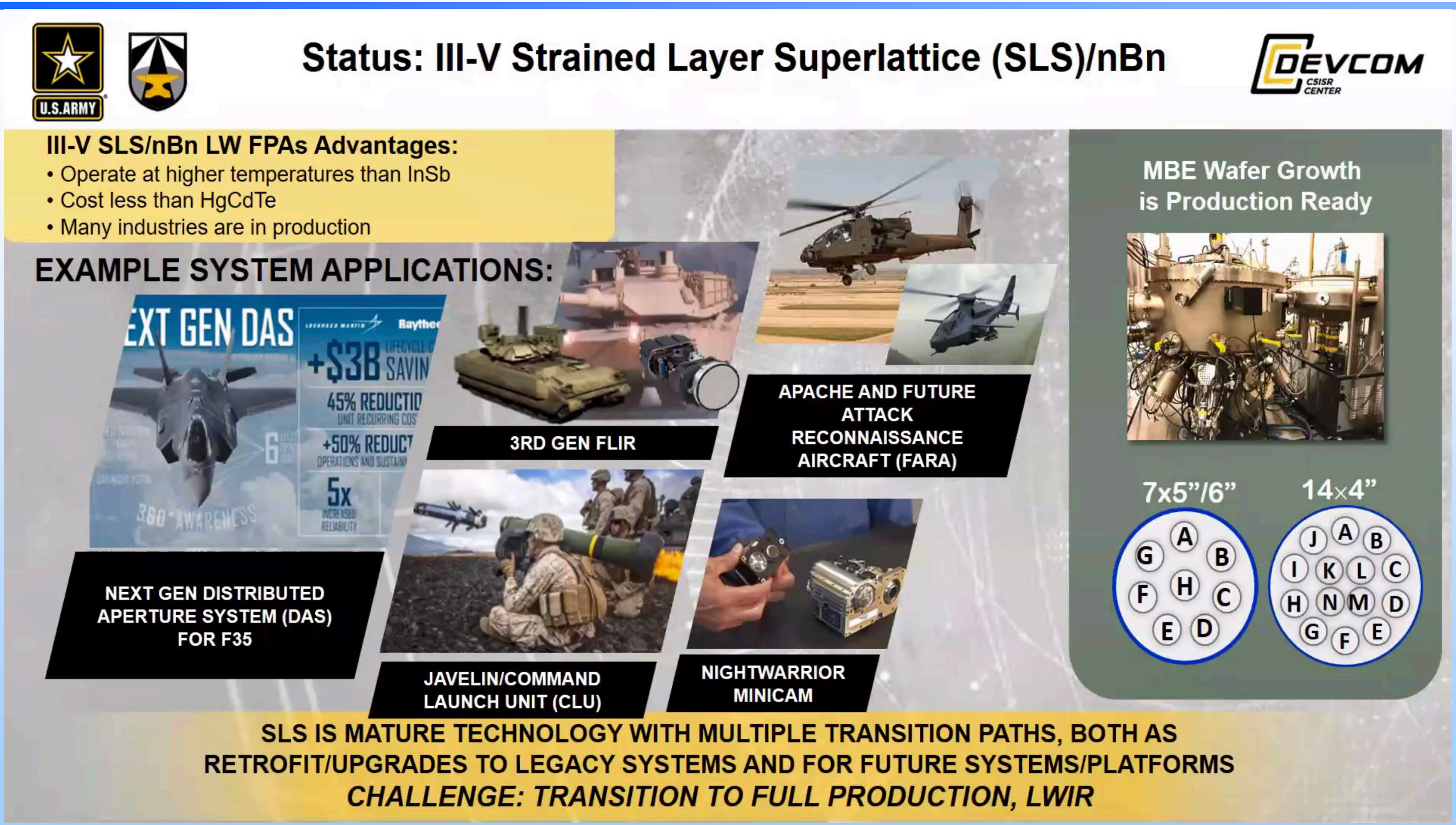

Reference: Donald A. Reago Jr., "Sensing for warfare in the digital information age," Proc. SPIE 11741, Infrared Technology and Applications XLVII, 1174103 (12 April 2021); https://doi.org/10.1117/12.2596793

Summary

- How T2SL FPAs have Changed the Infrared Landscape
  - Cross-cutting technology
  - Seven NASA funded instruments (**HyTI**, HyTES, HyTES-E, HyTI-2, c-FIRS, PIRS, MMI)

- What makes T2SL infrared FPAs attractive to Low SWaP instrument designers
  - Good QE; low dark current
  - High operating temperature
  - Low 1/f noise
  - High uniformity & pixel operability
  - Low cost
    - InAs/InAsSb T2SL; manufacturable
    - Readily available low cost GaSb substrate
    - Easily adaptable to the III-V fab lines

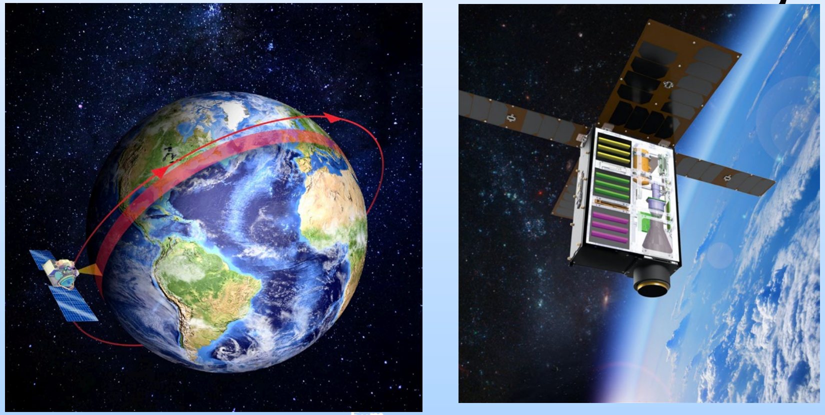

Artist rendering of c-FIRST & HyTI

Our work is sponsored by NASA, MDA, AFRL, AGA, VISTA, JPL R&TD, NASA ESTO under ACT, SLI-T InVEST, & IIP programs